

Lepton Flavor Universality tests through angular observables of $\bar{B} \rightarrow D^{(*)} \ell \bar{\nu}$ decay modes

DAMIR BEČIREVIĆ^a, MARCO FEDELE^b, IVAN NIŠANDŽIĆ^c, ANDREY TAYDUGANOV^d

^a *Laboratoire de Physique Théorique, Bât. 210 (UMR 8627)
Université Paris Sud, Université Paris-Saclay, 91405 Orsay cedex, France.*

^b *Departament de Física Quàntica i Astrofísica (FQA), Institut de Ciències del Cosmos (ICCUB), Universitat de Barcelona, Martí i Franquès 1, E08028 Barcelona, Spain.*

^c *Institut für Theoretische Teilchenphysik,
Karlsruher Institut für Technologie, Engesser-Str.7, D-76128 Karlsruhe, Germany.*

^d *Fakultät Physik, TU Dortmund, Otto-Hahn-Str.4, D-44221 Dortmund, Germany.*

Abstract

We discuss the possibility of using the observables deduced from the angular distribution of the $B \rightarrow D^{(*)} \ell \bar{\nu}$ decays to test the effects of lepton flavor universality violation (LFUV). We show that the measurement of even a subset of these observables could be very helpful in distinguishing the Lorentz structure of the New Physics contributions to these decays. To do so we use the low energy effective theory in which besides the Standard Model contribution we add all possible Lorentz structures with the couplings (Wilson coefficients) that are determined by matching theory with the measured ratios $R(D^{(*)})^{\text{exp}}$. We argue that even in the situation in which the measured $R(D^{(*)})^{\text{exp}}$ becomes fully compatible with the Standard Model, one can still have significant New Physics contributions the size of which could be probed by measuring the observables discussed in this paper and comparing them with their Standard Model predictions.

1 Introduction

Ever since the BaBar Collaboration reported on the first experimental indication of the lepton flavor universality violation (LFUV) in B -meson decays, after measuring the ratios [1, 2]

$$R(D^{(*)}) = \frac{\mathcal{B}(B \rightarrow D^{(*)}\tau\bar{\nu})}{\mathcal{B}(B \rightarrow D^{(*)}l\bar{\nu})} \Big|_{l \in \{e, \mu\}}, \quad (1)$$

we witnessed an intense activity in trying to understand why $R(D^{(*)})^{\text{SM}} < R(D^{(*)})^{\text{exp}}$, where SM stands for the theoretically established value in the Standard Model. Since then, the experimentalists at Belle and LHCb corroborated the tendency that indeed $R(D^{(*)})^{\text{SM}} < R(D^{(*)})^{\text{exp}}$ [3–6], while the theorists worked on scrutinizing the theoretical uncertainties within the SM [7–10] and proposed various models of New Physics (NP) that could accommodate the observed discrepancies [11–42]. The current values, including the most recent Belle result [43], are [44]:

$$R(D)^{\text{exp}} = 0.33(3), \quad R(D)^{\text{SM}} = 0.299(3), \quad (2)$$

$$R(D^*)^{\text{exp}} = 0.30(2), \quad R(D^*)^{\text{SM}} = 0.258(5), \quad (3)$$

which amounts to a combined 3.1σ disagreement between the measurements and the SM predictions. Measuring the ratios of similar decay rates is convenient because they are independent on the Cabibbo–Kobayashi–Maskawa (CKM) matrix element $|V_{cb}|$, and because of the cancellation of a significant amount of hadronic uncertainties. One should, however, be careful in assessing the uncertainties regarding the remaining non-perturbative QCD effects, especially in the case of $B \rightarrow D^*l\bar{\nu}_\ell$ ($\ell = e, \mu, \tau$) for which the information concerning the shapes of hadronic form factors has never been deduced from the results based on numerical simulations of QCD on the lattice.¹ In the case of $B \rightarrow D\ell\bar{\nu}_\ell$, instead, both the vector and scalar form factors have been computed on the lattice at several different $q^2 = (p_\ell + p_{\bar{\nu}_\ell})^2$ values [47–49]. Moreover, the theoretical studies reported in Ref. [50, 51] suggest that the soft photon radiation $B \rightarrow D\ell\bar{\nu}_\ell\gamma$ could be an important source of uncertainty in $R(D)^{\text{SM}}$, unaccounted for thus far. Further research in this direction is necessary and the associated theoretical uncertainty should be included in the overall error budget before the 5σ (or larger) discrepancy between theory (SM) and experiment is claimed.

Notice also that the LHCb Collaboration recently made another LFUV test based on $b \rightarrow c\ell\bar{\nu}_\ell$. They reported [52]

$$R(J/\psi) = \frac{\mathcal{B}(B_c \rightarrow J/\psi\tau\bar{\nu})}{\mathcal{B}(B_c \rightarrow J/\psi\mu\bar{\nu})} = 0.71 \pm 0.25, \quad (4)$$

¹Very recently the MILC collaboration presented preliminary results for the shapes of the $B \rightarrow D^*$ form factors [45, 46]. Numerical results, that could be used for phenomenology, are yet to be reported.

again about 2σ larger than predicted in the SM, $R(J/\psi)^{\text{SM}} < R(J/\psi)^{\text{exp}}$.

The above-mentioned experimental indications of LFUV have motivated many theorists to propose a scenario beyond the SM which could accommodate the measured values of $R(D^{(*)})$ and $R(J/\psi)$. In terms of a general low energy effective theory, which will be described in the next Section, the NP effects can show up at low energies through an enhancement of the contribution arising from either the (axial-)vector current-current operators, the (pseudo-)scalar operators, the tensor one, or from a combination of those [53–61]. Another important aspect in describing the LFUV effects in most of the models proposed so far is the assumption that the NP couplings involving τ are the source of LFUV, whereas those related to $l = e, \mu$ are much smaller and can be neglected. A rationale for that assumption is that the LFUV effects have not been observed in other semileptonic decay modes (which involve lighter mesons and light leptons). In addition to that, the results of a detailed angular analysis of $B \rightarrow D^{(*)}l\bar{\nu}_l$ [$l \in (e, \mu)$] by BaBar and by Belle were found to be fully consistent with the SM predictions. We will follow the same practice in this paper and assume that the deviations from the lepton flavor universality arise from the NP couplings to the third generation of leptons. We will formulate a general effective theory scenario for $b \rightarrow cl\bar{\nu}_l$ decays by adding all operators allowed by the CP and the Lorentz symmetries. In doing so we will not account for a possibility of the light right-handed neutrinos. Such models have been already proposed, but the problem they often encounter is that the NP amplitude does not interfere with the (dominant) SM one, and therefore getting $R(D^{(*)}) > R(D^{(*)})^{\text{SM}}$ compatible with $R(D^{(*)})^{\text{exp}}$ requires large NP couplings which could be in conflict with the bounds on these couplings that could be deduced from direct searches at the LHC.

Starting from the general effective theory we will provide the expressions for the full angular distribution of both decay processes, and then combine the coefficients involving the NP couplings in a number of observables. Some of these observables could be studied at the LHC, but most of them could be tested at Belle II. It is therefore reasonable to explore the possibilities of testing the effects of LFUV not only via the ratios of branching fractions [such as $R(D^{(*)})$], but also by using the ratios of these newly defined observables. Since various observables are sensitive to different NP operators, we will argue that the experimental analysis of the ratios we propose to study could indeed help disentangling the basic features of NP. We will then also provide a phenomenological analysis to illustrate our claim.

Before we embark on the details of this work we should emphasize that for the phenomenological analysis we need a full set of form factors (including the scalar, pseudoscalar and the tensor ones) computed by means of lattice QCD, which is not the case right now. A dedicated lattice computation of all the form factors relevant to $B \rightarrow D^{(*)}l\bar{\nu}_l$ is of great importance for a reliable assessment of LFUV. Since we have to make (reasonable) assumptions about the form factors, our phenomenological results should be understood as a diagnostic tool to distinguish among various Lorentz structures of the NP contributions,

while the accurate analysis will be possible only when the lattice QCD results become available.

The remainder of this paper is organized as follows: In Sec. 2 we provide the full angular distributions for both types of decays considered in this paper, and define all the observables which can be used to better test the effects of LFUV in these decays. In Sec. 3 we make the sensitivity study of the observables defined in Sec. 2 to the effects of LFUV, solely based on the deviations of the measured $R(D^{(*)})$ with respect to the SM predictions. We also made a short comment on the recently measured $F_L^{D^*}$. We finally summarize in Sec. 4. Several definitions and technical details are collected in the Appendices.

2 Full angular distributions of $\bar{B} \rightarrow D^{(*)} \ell \bar{\nu}$

In this Section we define the effective Hamiltonian for a generic NP scenario and then derive the expressions for the full angular distribution of the differential decay rate of $B \rightarrow D \ell \bar{\nu}_\ell$, and of $B \rightarrow D^*(\rightarrow D\pi) \ell \bar{\nu}_\ell$. All angular coefficients will be expressed in terms of helicity amplitudes which are properly defined in terms of kinematical variables and hadronic form factors. For the reader's convenience the decomposition of all the matrix elements in terms of form factors is provided in Appendix A of the present paper. With explicit expressions for the angular coefficients in hands, we will then proceed and define a set of observables that can be used to study the effects of LFUV.

2.1 Effective Hamiltonian

Assuming the neutrinos to be left-handed, the most general effective Hamiltonian describing the $b \rightarrow c \ell \bar{\nu}_\ell$ decays, containing all possible parity-conserving four-fermion dimension-6 operators, can be written as

$$\begin{aligned} \mathcal{H}_{\text{eff}} = \sqrt{2} G_F V_{cb} & \left[(1 + g_V) (\bar{c} \gamma_\mu b) (\bar{\ell}_L \gamma^\mu \nu_L) + (-1 + g_A) (\bar{c} \gamma_\mu \gamma_5 b) (\bar{\ell}_L \gamma^\mu \nu_L) \right. \\ & + g_S (\bar{c} b) (\bar{\ell}_R \nu_L) + g_P (\bar{c} \gamma_5 b) (\bar{\ell}_R \nu_L) \\ & \left. + g_T (\bar{c} \sigma_{\mu\nu} b) (\bar{\ell}_R \sigma^{\mu\nu} \nu_L) + g_{T5} (\bar{c} \sigma_{\mu\nu} \gamma_5 b) (\bar{\ell}_R \sigma^{\mu\nu} \nu_L) \right] + \text{h.c.} \end{aligned} \quad (5)$$

Note that we use the convention such that in the SM $g_i = 0$, $\forall i \in \{S, P, V, A, T, T5\}$.

It is often more convenient to write the above Hamiltonian in the chiral basis of operators,

$$\begin{aligned} \mathcal{H}_{\text{eff}} = \frac{4G_F}{\sqrt{2}} V_{cb} & \left[(1 + g_{V_L}) (\bar{c}_L \gamma_\mu b_L) (\bar{\ell}_L \gamma^\mu \nu_L) + g_{V_R} (\bar{c}_R \gamma_\mu b_R) (\bar{\ell}_L \gamma^\mu \nu_L) \right. \\ & + g_{S_L} (\bar{c}_R b_L) (\bar{\ell}_R \nu_L) + g_{S_R} (\bar{c}_L b_R) (\bar{\ell}_R \nu_L) \\ & \left. + g_{T_L} (\bar{c}_R \sigma_{\mu\nu} b_L) (\bar{\ell}_R \sigma^{\mu\nu} \nu_L) \right] + \text{h.c.}, \end{aligned} \quad (6)$$

which is obviously equivalent to Eq. (5), with the corresponding effective coefficients related as

$$g_{V,A} = g_{V_R} \pm g_{V_L}, \quad g_{S,P} = g_{S_R} \pm g_{S_L}, \quad g_T = -g_{T5} = g_{T_L}. \quad (7)$$

The last relation is also an easy way to see that $(\bar{c}_L \sigma_{\mu\nu} b_R)(\bar{\ell}_R \sigma^{\mu\nu} \nu_L)$, the right-handed tensor operator, cannot contribute to the decay amplitude.

2.2 $\bar{B} \rightarrow D \ell \bar{\nu}$ decay

We first focus on the decay to a pseudoscalar meson and write the differential decay rate as

$$\frac{d^2\Gamma}{dq^2 d\cos\theta_\ell} = \frac{\sqrt{\lambda_{BD}(q^2)}}{64(2\pi)^3 m_B^3} \left(1 - \frac{m_\ell^2}{q^2}\right) \sum_{\lambda_\ell} |\mathcal{M}^{\lambda_\ell}(\bar{B} \rightarrow D \ell \bar{\nu})|^2, \quad (8)$$

where we made use of the definition $\lambda_{BD}(q^2) = m_B^4 + m_D^4 + q^4 - 2(m_B^2 m_D^2 + m_B^2 q^2 + m_D^2 q^2)$. It is convenient to separate the angular from the q^2 dependence and write the above expression as

$$\frac{d^2\Gamma}{dq^2 d\cos\theta_\ell} = a_{\theta_\ell}(q^2) + b_{\theta_\ell}(q^2) \cos\theta_\ell + c_{\theta_\ell}(q^2) \cos^2\theta_\ell, \quad (9)$$

where θ_ℓ is the polar angle of the lepton momentum in the rest frame of the $\ell\bar{\nu}$ -pair with respect to the z axis which is defined by the D -momentum in the rest frame of \bar{B} . The corresponding angular coefficients can be written as

$$a_{\theta_\ell}(q^2) = \frac{G_F^2 |V_{cb}|^2}{256\pi^3 m_B^3} q^2 \sqrt{\lambda_{BD}(q^2)} \left(1 - \frac{m_\ell^2}{q^2}\right)^2 \left[|\tilde{h}_0^-|^2 + \frac{m_\ell^2}{q^2} |\tilde{h}_t|^2 \right], \quad (10a)$$

$$b_{\theta_\ell}(q^2) = \frac{G_F^2 |V_{cb}|^2}{128\pi^3 m_B^3} q^2 \sqrt{\lambda_{BD}(q^2)} \left(1 - \frac{m_\ell^2}{q^2}\right)^2 \frac{m_\ell^2}{q^2} \mathcal{R}e[\tilde{h}_0^+ \tilde{h}_t^*], \quad (10b)$$

$$c_{\theta_\ell}(q^2) = -\frac{G_F^2 |V_{cb}|^2}{256\pi^3 m_B^3} q^2 \sqrt{\lambda_{BD}(q^2)} \left(1 - \frac{m_\ell^2}{q^2}\right)^2 \left[|\tilde{h}_0^-|^2 - \frac{m_\ell^2}{q^2} |\tilde{h}_0^+|^2 \right], \quad (10c)$$

where $\tilde{h}_\lambda^{\lambda_\ell}$ are the linear combinations of the “*standard*” hadronic helicity amplitudes which are defined and computed in Appendix B of the present paper.

Integration over the polar angle θ_ℓ leads to the expression for the differential decay rate,

$$\begin{aligned} \frac{d\Gamma}{dq^2} &= 2a_{\theta_\ell}(q^2) + \frac{2}{3}c_{\theta_\ell}(q^2) \\ &= \frac{G_F^2 |V_{cb}|^2}{192\pi^3 m_B^3} q^2 \sqrt{\lambda_{BD}(q^2)} \left(1 - \frac{m_\ell^2}{q^2}\right)^2 \times \left\{ |\tilde{h}_0^-|^2 + \frac{m_\ell^2}{2q^2} |\tilde{h}_0^+|^2 + \frac{3}{2} \frac{m_\ell^2}{q^2} |\tilde{h}_t|^2 \right\}. \end{aligned} \quad (11)$$

We see that the linear dependence on $\cos\theta_\ell$ in Eq. (9) is lost after integration in θ_ℓ , but it can be recovered by considering the forward-backward asymmetry,

$$\mathcal{A}_{\text{FB}}(q^2) = \frac{\int_0^1 \frac{d^2\Gamma}{dq^2 d\cos\theta_\ell} d\cos\theta_\ell - \int_{-1}^0 \frac{d^2\Gamma}{dq^2 d\cos\theta_\ell} d\cos\theta_\ell}{d\Gamma/dq^2} = \frac{b_{\theta_\ell}(q^2)}{d\Gamma/dq^2}. \quad (12)$$

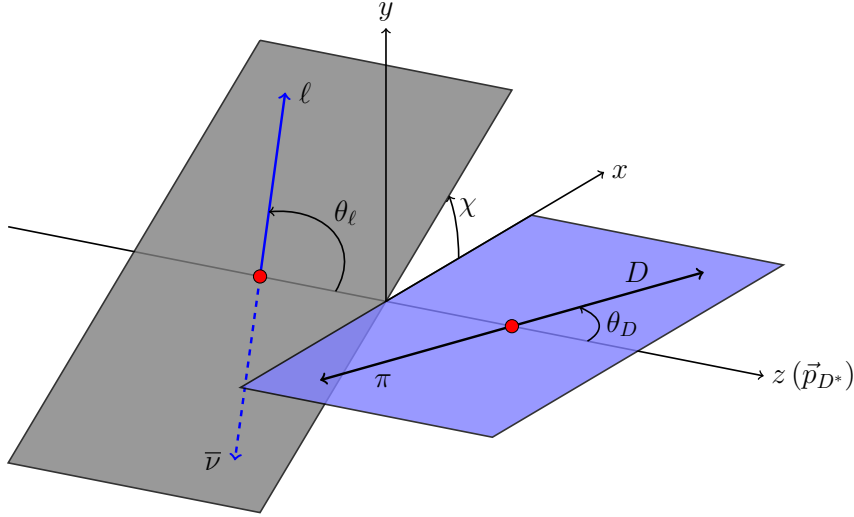


Figure 1: Kinematics of the $\bar{B} \rightarrow D^*(\rightarrow D\pi)\ell\bar{\nu}$ decay.

Another interesting observable for the study of the NP effects is the lepton polarization asymmetry defined from differential decay rates with definite lepton helicity:

$$\frac{d\Gamma^{\lambda_\ell=+1/2}}{dq^2} = \frac{G_F^2 |V_{cb}|^2}{192\pi^3 m_B^3} q^2 \sqrt{\lambda_{BD}(q^2)} \left(1 - \frac{m_\ell^2}{q^2}\right)^2 \frac{m_\ell^2}{2q^2} \left[|\tilde{h}_0^+|^2 + 3|\tilde{h}_t|^2 \right], \quad (13a)$$

$$\frac{d\Gamma^{\lambda_\ell=-1/2}}{dq^2} = \frac{G_F^2 |V_{cb}|^2}{192\pi^3 m_B^3} q^2 \sqrt{\lambda_{BD}(q^2)} \left(1 - \frac{m_\ell^2}{q^2}\right)^2 |\tilde{h}_0^-|^2. \quad (13b)$$

The corresponding polarization asymmetry reads

$$\mathcal{A}_{\lambda_\ell}(q^2) = \frac{d\Gamma^{\lambda_\ell=-1/2}/dq^2 - d\Gamma^{\lambda_\ell=+1/2}/dq^2}{d\Gamma/dq^2} = 1 - 2 \frac{d\Gamma^{\lambda_\ell=+1/2}/dq^2}{d\Gamma/dq^2}. \quad (14)$$

2.3 $\bar{B} \rightarrow D^*(\rightarrow D\pi)\ell\bar{\nu}$ decay

We now discuss the case of the \bar{B} -meson decaying to the vector meson in the final state. In this work, for the computation of the helicity amplitudes and differential decay rates, we define the system of coordinates as depicted in Fig. 1: the z -axis is set along the D^* momentum in the \bar{B} rest frame, and the x -axis is chosen in a way that the D momentum in the D^* rest frame lies in the $x-z$ plane and has the positive x -component.

The full angular distribution reads,

$$\frac{d^5\Gamma}{dq^2 dm_{D\pi}^2 d\cos\theta_D d\cos\theta_\ell d\chi} = \frac{\sqrt{\lambda_{BD^*}(q^2)}}{256(2\pi)^6 m_B^3} \left(1 - \frac{m_\ell^2}{q^2}\right) \frac{|\hat{\mathbf{p}}_D|}{m_{D\pi}} \sum_{\lambda_\ell} \left| \sum_{\lambda_{D^*}} \mathcal{M}^{\lambda_{D^*}, \lambda_\ell}(\bar{B} \rightarrow D\pi\ell\bar{\nu}_\ell) \right|^2, \quad (15)$$

where again $\lambda_{BD^*}(q^2) = m_B^4 + m_{D^*}^4 + q^4 - 2(m_B^2 m_{D^*}^2 + m_B^2 q^2 + m_{D^*}^2 q^2)$, and

$$|\hat{\mathbf{p}}_D| = \frac{\sqrt{\lambda(m_{D\pi}^2, m_D^2, m_\pi^2)}}{2m_{D\pi}}. \quad (16)$$

After integrating over $m_{D\pi}^2$ around the D^* -resonance, the above distribution becomes

$$\begin{aligned} \frac{d^4\Gamma}{dq^2 d\cos\theta_D d\cos\theta_\ell d\chi} = \frac{9}{32\pi} \bigg\{ & I_{1c} \cos^2\theta_D + I_{1s} \sin^2\theta_D \\ & + [I_{2c} \cos^2\theta_D + I_{2s} \sin^2\theta_D] \cos 2\theta_\ell \\ & + [I_{6c} \cos^2\theta_D + I_{6s} \sin^2\theta_D] \cos\theta_\ell \\ & + [I_3 \cos 2\chi + I_9 \sin 2\chi] \sin^2\theta_\ell \sin^2\theta_D \\ & + [I_4 \cos\chi + I_8 \sin\chi] \sin 2\theta_\ell \sin 2\theta_D \\ & + [I_5 \cos\chi + I_7 \sin\chi] \sin\theta_\ell \sin 2\theta_D \bigg\}, \end{aligned} \quad (17)$$

where the angular coefficients $I_i \equiv I_i(q^2)$ are given by:

$$I_{1c} = 2N \left[|\tilde{H}_0^-|^2 + \frac{m_\ell^2}{q^2} |\tilde{H}_0^+|^2 + 2\frac{m_\ell^2}{q^2} |\tilde{H}_t|^2 \right], \quad (18a)$$

$$I_{1s} = \frac{N}{2} \left[3(|\tilde{H}_+^-|^2 + |\tilde{H}_-^-|^2) + \frac{m_\ell^2}{q^2} (|\tilde{H}_+^+|^2 + |\tilde{H}_-^+|^2) \right], \quad (18b)$$

$$I_{2c} = 2N \left[-|\tilde{H}_0^-|^2 + \frac{m_\ell^2}{q^2} |\tilde{H}_0^+|^2 \right], \quad (18c)$$

$$I_{2s} = \frac{N}{2} \left[|\tilde{H}_+^-|^2 + |\tilde{H}_-^-|^2 - \frac{m_\ell^2}{q^2} (|\tilde{H}_+^+|^2 + |\tilde{H}_-^+|^2) \right], \quad (18d)$$

$$I_3 = -2N \operatorname{Re} \left[\tilde{H}_+^- \tilde{H}_-^{*-} - \frac{m_\ell^2}{q^2} \tilde{H}_+^+ \tilde{H}_-^{*+} \right] = -2N\beta_\ell^2 \operatorname{Re} [H_+ H_-^* - 4H_{T,+} H_{T,-}^*], \quad (18e)$$

$$\begin{aligned} I_4 &= N \operatorname{Re} \left[(\tilde{H}_+^- + \tilde{H}_-^-) \tilde{H}_0^{-*} - \frac{m_\ell^2}{q^2} (\tilde{H}_+^+ + \tilde{H}_-^+) \tilde{H}_0^{*+} \right] \\ &= N\beta_\ell^2 \operatorname{Re} [(H_+ + H_-) H_0^* - 4(H_{T,+} + H_{T,-}) H_{T,0}^*], \end{aligned} \quad (18f)$$

$$I_5 = 2N \operatorname{Re} \left[(\tilde{H}_+^- - \tilde{H}_-^-) \tilde{H}_0^{-*} - \frac{m_\ell^2}{q^2} (\tilde{H}_+^+ + \tilde{H}_-^+) \tilde{H}_t^* \right], \quad (18g)$$

$$I_{6c} = 8N \frac{m_\ell^2}{q^2} \mathcal{R}e[\tilde{H}_0^+ \tilde{H}_t^*], \quad (18h)$$

$$I_{6s} = 2N(|\tilde{H}_+^-|^2 - |\tilde{H}_-^-|^2), \quad (18i)$$

$$I_7 = 2N \mathcal{I}m \left[(\tilde{H}_+^- + \tilde{H}_-^-) \tilde{H}_0^{-*} - \frac{m_\ell^2}{q^2} (\tilde{H}_+^+ - \tilde{H}_-^+) \tilde{H}_t^* \right], \quad (18j)$$

$$\begin{aligned} I_8 &= N \mathcal{I}m \left[(\tilde{H}_+^- - \tilde{H}_-^-) \tilde{H}_0^{-*} - \frac{m_\ell^2}{q^2} (\tilde{H}_+^+ - \tilde{H}_-^+) \tilde{H}_0^{+*} \right] \\ &= N\beta_\ell^2 \mathcal{I}m [(H_+ - H_-) H_0^* - 4(H_{T,+} - H_{T,-}) H_{T,0}^*], \end{aligned} \quad (18k)$$

$$I_9 = -2N \mathcal{I}m \left[\tilde{H}_+^- \tilde{H}_-^{-*} - \frac{m_\ell^2}{q^2} \tilde{H}_+^+ \tilde{H}_-^{+*} \right] = -2N\beta_\ell^2 \mathcal{I}m [H_+ H_-^* - 4H_{T,+} H_{T,-}^*], \quad (18l)$$

with

$$N \equiv N(q^2) = \mathcal{B}(D^* \rightarrow D\pi) \frac{G_F^2 |V_{cb}|^2}{48(2\pi)^3 m_B^3} q^2 \sqrt{\lambda_{BD^*}(q^2)} \left(1 - \frac{m_\ell^2}{q^2}\right)^2. \quad (19)$$

The explicit expressions for the hadronic helicity amplitudes H_λ , as well as their linear combinations $\tilde{H}_\lambda^{\lambda_\ell}$, are given in Appendix B.

It is now possible to write down three partially integrated decay distributions, integrating all but one angle at a time.

- θ_ℓ distribution :

$$\begin{aligned} \frac{d^2\Gamma}{dq^2 d \cos \theta_\ell} &= a_{\theta_\ell}(q^2) + b_{\theta_\ell}(q^2) \cos \theta_\ell + c_{\theta_\ell}(q^2) \cos^2 \theta_\ell, \\ a_{\theta_\ell}(q^2) &= \frac{3}{8} (I_{1c} + 2I_{1s} - I_{2c} - 2I_{2s}), \\ b_{\theta_\ell}(q^2) &= \frac{3}{8} (I_{6c} + 2I_{6s}), \\ c_{\theta_\ell}(q^2) &= \frac{3}{4} (I_{2c} + 2I_{2s}). \end{aligned} \quad (20)$$

- θ_D distribution :

$$\begin{aligned} \frac{d^2\Gamma}{dq^2 d \cos \theta_D} &= a_{\theta_D}(q^2) + c_{\theta_D}(q^2) \cos^2 \theta_D, \\ a_{\theta_D}(q^2) &= \frac{3}{8} (3I_{1s} - I_{2s}), \\ c_{\theta_D}(q^2) &= \frac{3}{8} (3I_{1c} - 3I_{1s} - I_{2c} + I_{2s}). \end{aligned} \quad (21)$$

- χ distribution :

$$\begin{aligned}\frac{d^2\Gamma}{dq^2 d\chi} &= a_\chi(q^2) + c_\chi^c(q^2) \cos 2\chi + c_\chi^s(q^2) \sin 2\chi, \\ a_\chi(q^2) &= \frac{1}{8\pi} (3I_{1c} + 6I_{1s} - I_{2c} - 2I_{2s}) \\ c_\chi^c(q^2) &= \frac{1}{2\pi} I_3, \\ c_\chi^s(q^2) &= \frac{1}{2\pi} I_9.\end{aligned}\tag{22}$$

Illustration of the q^2 -dependence of the above observables, for fixed values of g_i 's, is provided in Fig. 2.

It is interesting to point out that the terms proportional to $\cos \theta_D$, $\cos \chi$ and $\sin \chi$ are absent in the distributions written above. Such terms can arise if a non-zero interference with the S -wave contribution, $\bar{B} \rightarrow (D\pi)_S \ell \bar{\nu}$, is included in the distribution, as discussed in Ref. [56].

2.3.1 Observables

From the full angular distribution (17) we isolate various coefficients and combine them into various quantities normalized to the differential decay rate. In the following we define 12 such quantities with a goal to use them in order to scrutinize the effects of LFUV that we propose to study. When necessary, before defining an observable, we will indicate how the corresponding coefficients can be isolated from the full angular distribution.

- Differential decay rate

$$\frac{d\Gamma}{dq^2} = \frac{1}{4} (3I_{1c} + 6I_{1s} - I_{2c} - 2I_{2s}),\tag{23}$$

- Forward-backward asymmetry

$$\mathcal{A}_{\text{FB}}(q^2) = \frac{b_{\theta_\ell}(q^2)}{d\Gamma/dq^2} = \frac{3(I_{6c} + 2I_{6s})}{8 d\Gamma/dq^2},\tag{24}$$

- Lepton polarization asymmetry

$$\mathcal{A}_{\lambda_\ell}(q^2) = \frac{d\Gamma^{\lambda_\ell=-1/2}/dq^2 - d\Gamma^{\lambda_\ell=+1/2}/dq^2}{d\Gamma/dq^2},\tag{25}$$

with

$$\begin{aligned}\frac{d\Gamma^{\lambda_\ell=+1/2}}{dq^2} &= \frac{1}{4} (I_{1c} + 2I_{1s} + I_{2c} - 6I_{2s}) + I_n \\ \frac{d\Gamma^{\lambda_\ell=-1/2}}{dq^2} &= \frac{1}{2} (I_{1c} + 2I_{1s} - I_{2c} + 2I_{2s}) - I_n,\end{aligned}\tag{26}$$

where we introduced an additional coefficient

$$I_n = 2N \frac{m_\ell^2}{q^2} |\tilde{H}_t|^2, \quad (27)$$

which is not present in Eq. (17) because in the full angular distribution we have summed over the lepton polarization states.

- D^* polarization fraction

$$R_{L,T}(q^2) = \frac{d\Gamma_{L,T}/dq^2}{d\Gamma_T/dq^2}, \quad (28)$$

where Γ_L and Γ_T represent the longitudinal and transverse D^* polarization decay rates,

$$\begin{aligned} \frac{d\Gamma_L}{dq^2} &= \frac{2}{3} [a_{\theta_D}(q^2) + c_{\theta_D}(q^2)] = \frac{1}{4} (3I_{1c} - I_{2c}), \\ \frac{d\Gamma_T}{dq^2} &= \frac{4}{3} a_{\theta_D}(q^2) = \frac{1}{2} (3I_{1s} - I_{2s}). \end{aligned} \quad (29)$$

Alternatively, one can define the quantity $F_L^{D^*}$ which is a measure of the longitudinally polarized D^* 's in the whole ensemble of $\bar{B} \rightarrow D^* \ell \bar{\nu}$ decays, which is related to $R_{L,T}(q^2)$ as:

$$F_L^{D^*}(q^2) = \frac{R_{L,T}(q^2)}{1 + R_{L,T}(q^2)} = \frac{1}{2} \frac{3I_{1c} - I_{2c}}{3(I_{1c} + I_{1s}) - I_{2c} - I_{2s}}. \quad (30)$$

$F_L^{D^*}$ is often referred to as $F_L^{D^*}(q^2)$ integrated over the available phase space.

- $R_{A,B}$

$$R_{A,B}(q^2) = \frac{d\Gamma_A/dq^2}{d\Gamma_B/dq^2}, \quad (31)$$

$$\begin{aligned} \frac{d\Gamma_A}{dq^2} &= \frac{2}{3} [a_{\theta_\ell}(q^2) - c_{\theta_\ell}(q^2)] = \frac{1}{4} (I_{1c} + 2I_{1s} - 3I_{2c} - 6I_{2s}), \\ \frac{d\Gamma_B}{dq^2} &= \frac{4}{3} [a_{\theta_\ell}(q^2) + c_{\theta_\ell}(q^2)] = \frac{1}{2} (I_{1c} + 2I_{1s} + I_{2c} + 2I_{2s}) = \frac{d\Gamma}{dq^2} - \frac{d\Gamma_A}{dq^2}. \end{aligned} \quad (32)$$

- A_3 and A_9

$$\begin{aligned} A_3(q^2) &= \frac{c_\chi^c(q^2)}{d\Gamma/dq^2} = \frac{1}{2\pi} \frac{I_3}{d\Gamma/dq^2}, \\ A_9(q^2) &= \frac{c_\chi^s(q^2)}{d\Gamma/dq^2} = \frac{1}{2\pi} \frac{I_9}{d\Gamma/dq^2}. \end{aligned} \quad (33)$$

- A_4 and A_8

If, from the full angular distribution, we first define the auxiliary quantities:

$$\begin{aligned}\Phi_{48}(q^2, \chi, \theta_\ell) &= \left[\int_{-1}^0 - \int_0^1 \right] \frac{d^4\Gamma}{dq^2 d\chi d \cos \theta_\ell d \cos \theta_D} d \cos \theta_D \\ \tilde{\Phi}_{48}(q^2, \chi) &= \left[\int_{-1}^0 - \int_0^1 \right] \Phi_{48}(q^2, \chi, \theta_\ell) d \cos \theta_\ell,\end{aligned}\quad (34)$$

then we can extract another two observables as,

$$\begin{aligned}A_4(q^2) &= \frac{\left[\int_{\pi/2}^{3\pi/2} - \int_0^{\pi/2} - \int_{3\pi/2}^{2\pi} \right] \tilde{\Phi}_{48}(q^2, \chi) d\chi}{d\Gamma/dq^2} = -\frac{2}{\pi} \frac{I_4}{d\Gamma/dq^2}. \\ A_8(q^2) &= \frac{\left[\int_0^\pi - \int_\pi^{2\pi} \right] \tilde{\Phi}_{48}(q^2, \chi) d\chi}{d\Gamma/dq^2} = \frac{2}{\pi} \frac{I_8}{d\Gamma/dq^2}.\end{aligned}\quad (35)$$

- A_5 and A_7

Similarly, if one first defines the asymmetry of the full angular distribution with respect to θ_D , namely,

$$\Phi_{57}(q^2, \chi) = \left[\int_{-1}^0 - \int_0^1 \right] \frac{d^3\Gamma}{dq^2 d\chi d \cos \theta_D} d \cos \theta_D, \quad (36)$$

one can define two additional observables as follows:

$$\begin{aligned}A_5(q^2) &= -\frac{\left[\int_{\pi/2}^{3\pi/2} - \int_0^{\pi/2} - \int_{3\pi/2}^{2\pi} \right] \Phi_{57}(q^2, \chi) d\chi}{d\Gamma/dq^2} = -\frac{3}{4} \frac{I_5}{d\Gamma/dq^2}, \\ A_7(q^2) &= \frac{\left[\int_0^\pi - \int_\pi^{2\pi} \right] \Phi_{57}(q^2, \chi) d\chi}{d\Gamma/dq^2} = -\frac{3}{4} \frac{I_7}{d\Gamma/dq^2}.\end{aligned}\quad (37)$$

- A_{6s}

Finally from the asymmetry with respect to θ_ℓ .

$$\Phi_6(q^2, \theta_D) = \left[\int_{-1}^0 - \int_0^1 \right] \frac{d^3\Gamma}{dq^2 d \cos \theta_D d \cos \theta_\ell} d \cos \theta_\ell, \quad (38)$$

we can isolate a term proportional to I_{6s} as

$$A_{6s}(q^2) = \frac{\left[7 \int_{-1/2}^{1/2} - \int_{1/2}^1 - \int_{-1}^{-1/2} \right] \Phi_6(q^2, \theta_D) d \cos \theta_D}{d\Gamma/dq^2} = -\frac{27}{8} \frac{I_{6s}}{d\Gamma/dq^2}. \quad (39)$$

In the above definitions we played with Eq. (17) to isolate each of the angular coefficients $I_i \equiv I_i(q^2)$. Alternatively, with a large enough sample one can fit the full data set to Eq. (17) and extract each of the coefficients with respect to the full (differential) decay rate. The SM values of all

$$\langle I_i \rangle_\ell = \frac{1}{\Gamma(B \rightarrow D^* \ell \bar{\nu}_\ell)} \times \int_{m_\ell^2}^{(m_B - m_{D^*})^2} I_i^\ell(q^2) dq^2 \quad (40)$$

for each of the leptons in the final state, are given in Tab. 1.

ℓ	$\langle I_{1c} \rangle_\ell$	$\langle I_{1s} \rangle_\ell$	$\langle I_{2c} \rangle_\ell$	$\langle I_{2s} \rangle_\ell$	$\langle I_3 \rangle_\ell$	$\langle I_4 \rangle_\ell$	$\langle I_5 \rangle_\ell$	$\langle I_{6c} \rangle_\ell$	$\langle I_{6s} \rangle_\ell$	$\langle I_7 \rangle_\ell$	$\langle I_8 \rangle_\ell$	$\langle I_9 \rangle_\ell$
e	0.521(2)	0.359(2)	-0.520(2)	0.120(1)	-0.170(3)	-0.304(1)	0.26(1)	0	-0.32(1)	0	0	0
μ	0.524(2)	0.359(2)	-0.510(2)	0.119(1)	-0.170(3)	-0.302(1)	0.26(1)	0.014(1)	-0.32(1)	0	0	0
τ	0.56(1)	0.379(4)	-0.166(2)	0.064(1)	-0.105(1)	-0.138(1)	0.299(5)	0.36(2)	-0.26(1)	0	0	0

Table 1: *Standard Model values of the coefficients appearing in the angular distribution (17), integrated over the full available phase space, as indicated in Eq. (40). The values are obtained by using the form factors that are in the text referred to as CLN+HQET.*

The example plots of q^2 -dependent observables for different benchmark values of NP couplings are depicted in Fig. 2.

2.4 Testing LFUV through angular observables

One can now make the ratios between the above observables with the τ -lepton in the final state and the same observables extracted from the decay to l [$l \in (e, \mu)$]. Of course this can only be done for the quantities which are nonzero in the SM. For the observables proportional to $I_{7,8,9}$, which are zero in the SM, we consider the differences, namely

$$D(A_{7,8,9}) \equiv \langle A_{7,8,9}^\tau \rangle - \frac{1}{2} \left(\langle A_{7,8,9}^e \rangle + \langle A_{7,8,9}^\mu \rangle \right). \quad (41)$$

For all the other observables, defined in Eqs. (12), (14) and (24)–(39), we define the LFUV observables as:

$$R(O_i) \equiv \frac{\langle O_i^\tau \rangle}{\frac{1}{2} (\langle O_i^e \rangle + \langle O_i^\mu \rangle)}, \quad (42)$$

where each O_i^ℓ is integrated over the available phase space. The only exception to this definition is made in the case of $\mathcal{A}_{\text{FB}}^D$ which we divide by m_ℓ^2 in order to make the effect of the presence of NP more pronounced.² Since most of the observables are written in terms

²In other words, $R(\mathcal{A}_{\text{FB}}^D) = \langle \mathcal{A}_{\text{FB}}^{D\tau} / m_\tau^2 \rangle / \left(1/2 \times \langle \mathcal{A}_{\text{FB}}^{D\mu} / m_\mu^2 \rangle + 1/2 \times \langle \mathcal{A}_{\text{FB}}^{De} / m_e^2 \rangle \right)$.

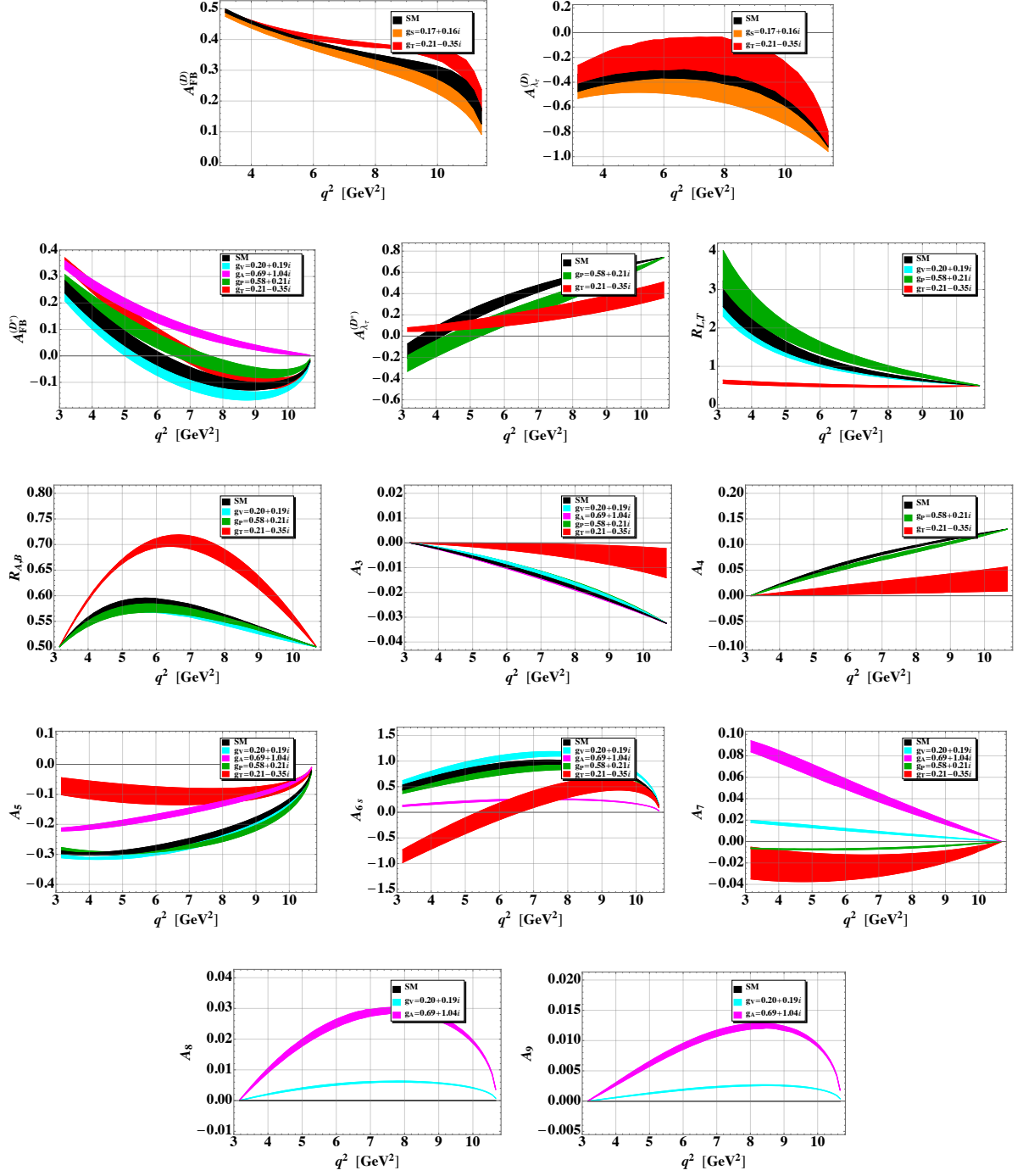


Figure 2: A_{FB} , A_{λ_τ} observables relevant to $\bar{B} \rightarrow D\tau\bar{\nu}$ and A_{FB} , A_{λ_τ} , $R_{L,T}$, $R_{A,B}$ and A_{3-9} relevant to $\bar{B} \rightarrow D^*\tau\bar{\nu}$ are displayed for various values of NP couplings and as functions of q^2 . The width of each curve comes from the theoretical uncertainties in hadronic form factors and quark masses. The benchmark g_i 's are chosen to be the best fit values, as discussed in the text.

of the ratios, $O_i^\ell(q^2) = \mathcal{N}_i^\ell(q^2)/\mathcal{D}_i^\ell(q^2)$ with \mathcal{N} and \mathcal{D} being generically a numerator and a denominator, the integrated quantities are then defined as

$$\langle O_i^\ell \rangle = \frac{\int_{m_i^2}^{q_{\max}^2} \mathcal{N}_i^\ell(q^2) dq^2}{\int_{m_i^2}^{q_{\max}^2} \mathcal{D}_i^\ell(q^2) dq^2}. \quad (43)$$

As it can be seen from the previous subsections, most of the observables are normalized to the differential decay rate which makes it difficult to monitor a dependence on $g_{V,A,V_L} \neq 0$, since the dependence on these couplings would cancel in these observables. Since in many specific models it is proposed to accommodate $R(D^{(*)})^{\text{exp}} > R(D^{(*)})^{\text{SM}}$ by switching on $g_{V_L} \neq 0$, the only departure from the SM value would indeed be in $R(D^{(*)})$, while all the other observables would remain compatible with the SM predictions.

3 Sensitivity to New Physics

To study the sensitivity of the LFUV observables defined in the previous Section on the non-zero values of g_i 's, we determine possible values of g_i 's from the fit to the measured $R(D)$ and $R(D^*)$. To do so we use the publicly available code `HEPfit` [62] in which the Bayesian statistical approach is adopted.

Since the hadronic uncertainties are the main source of the theoretical error, we have to be careful regarding the dependence of observables on the choice of form factors. In that respect we first used the set of form factors obtained in the constituent quark model of Ref. [63] which contains all of the form factors needed for this study. The uncertainties of the results obtained by the quark models are, however, unclear and attributing 10% uncertainty to each of the form factors is just an educated guess derived from the comparison between the predicted and measured decay rates. For that reason the results obtained by using the quark model form factors could only be considered as qualitative and the departures from the SM predictions only as indication (diagnostic) of the presence of LFUV.

Another choice of form factors consists in relying on the experimental analyses of the angular distribution of $\bar{B} \rightarrow D^* l \bar{\nu}$ [$l \in (e, \mu)$] decays from which the ratios of form factors can be extracted if one assumes the so called CLN parametrization of the dominant form factor $A_1(q^2)$ [64]. The experimental averages of the corresponding parameters [ρ^2 , $R_1(1)$, $R_2(1)$] and the information about their correlations is provided by HFLAV [44] and we use it in this work.³ As for the remaining form factors we used the expressions derived in

³Notice that the HFLAV results are obtained by using the CLN parametrization which fit well the data. Recent studies [10] show that the so called BGL parametrization of Ref. [65] should be preferred because the slopes of the ratios $R_{1,2}(w)$ are not fixed, but left as free parameters. In Ref. [66] it was shown,

heavy quark effective theory (HQET) [8] in which the leading α_s and the leading power corrections have been included to compute A_0/A_1 , f_T/f_+ , $T_{1,2,3}/A_1$ to each of which we attribute 10% of error (considerably larger than those quoted in Ref. [8]). Finally, for the form factors f_+ and f_0 we use the results obtained in numerical simulations of QCD on the lattice [68]. We have checked that our final results obtained by using the form factors computed in the constituent quark model of Ref. [63] are practically indistinguishable from those obtained with the form factors chosen as explained in this paragraph to which we will refer as “CLN+HQET+LATT”. Since less assumptions are needed in the error estimate of the form factors in the latter case, in the following all our results will be obtained by choosing CLN+HQET+LATT form factors [8, 44, 64, 68].

We now proceed and allow for one complex valued coefficient g_i to be non-zero at a time, i.e. we add 2 extra parameters (compared to the SM case) in every fit. We emphasize once again that we assume the NP to affect only the decay modes with τ in the final state, namely, $\bar{B} \rightarrow D^{(*)}\tau\bar{\nu}_\tau$. The joint *probability distribution functions* (*p.d.f.*’s) for the coefficients g_i are therefore obtained by using $R(D)^{\text{exp}}$ and $R(D^*)^{\text{exp}}$ as constraint, and then they are employed to predict all of the LFUV observables discussed in the previous Section. From the comparison with the SM results we can see which quantity is more sensitive to the considered $g_i \neq 0$. Notice again that the $B \rightarrow D\tau\nu_\tau$ observables will be affected by NP effects in $g_{V,S,T}$, while $g_{V,A,P,T} \neq 0$ will modify the $B \rightarrow D^*\tau\nu_\tau$ ones.

3.1 Fit results

In Fig. 3 and 4 we show the allowed regions for the NP couplings g_i relevant to the basis (5) and (6), respectively. We reiterate that the allowed regions for NP couplings are obtained by letting one (complex valued) coupling g_i to be non-zero at a time. Any value of the g_i derived in this way is plausible. We also include the limit derived from the B_c -meson lifetime as discussed in Refs. [69, 70] which is particularly restrictive to the pseudoscalar NP contribution g_P , as well as in g_{S_L, S_R} . In this paper we take the conservative limit $\mathcal{B}(B_c \rightarrow \tau\bar{\nu}) \lesssim 30\%$ and use the expression

$$\mathcal{B}(B_c \rightarrow \tau\bar{\nu}) = \tau_{B_c} \frac{m_{B_c} f_{B_c}^2 G_F^2 |V_{cb}|^2}{8\pi} m_\tau^2 \left(1 - \frac{m_\tau^2}{m_{B_c}^2}\right)^2 \left|1 + g_{V_L} + \frac{(g_{S_R} - g_{S_L}) m_{B_c}^2}{m_\tau(m_b + m_c)}\right|^2, \quad (44)$$

where the B_c decay constant $f_{B_c} = 427(6)$ MeV has been determined in the lattice QCD study of Ref. [71].

however, that both parametrizations provide good fit with data. The resulting $|V_{cb}|$ values, as obtained from fitting the data to these two parametrizations, were different. Since we are not interested in assessing the value of $|V_{cb}|$, the choice of parametrization is immaterial. Notice, however, that the most recent study by Belle [67] in which a larger sample of data has been used, showed that (a) the form factor shapes are fully consistent with the results reported by HFLAV [44], and (b) the values of $|V_{cb}|$ inferred from the fits to two parametrizations (CLN and BGL) are consistent with each other, both being lower than $|V_{cb}|$ extracted from the inclusive decays.

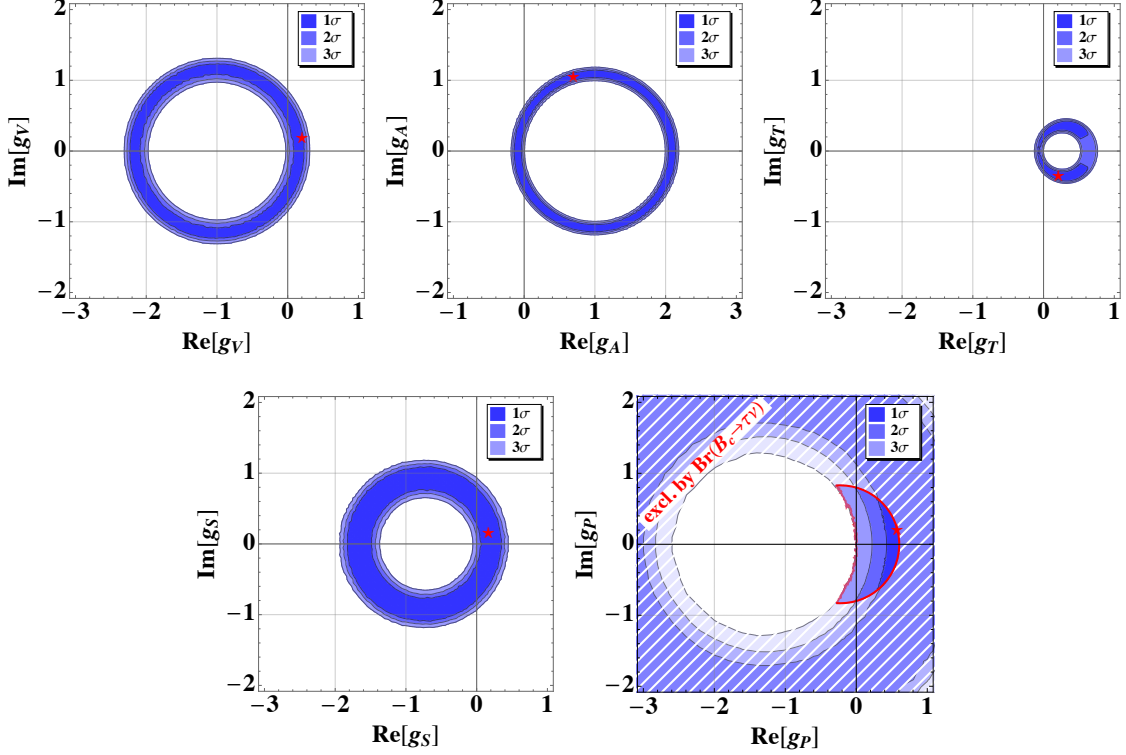


Figure 3: The allowed values for the NP couplings in Eq. (5) as obtained from the fit with $R(D)^{\text{exp}}$ and $R(D^*)^{\text{exp}}$, and by switching one coupling g_i at the time. Red stars denote the best fit values. Regarding the form factors we used those to which we refer in the text as CLN+HQET+LATT.

The benchmark values, denoted by red stars in Figs. 3-4, correspond to the best fit values. We get

$$\begin{aligned}
 g_V &= 0.20 + i 0.19, & g_A &= 0.69 + i 1.04, \\
 g_S &= 0.17 + i 0.16, & g_P &= 0.58 + i 0.21, & g_T - g_{T5} &= 0.21 - i 0.35,
 \end{aligned}
 \tag{45}$$

and in terms of couplings introduced in Eq. (6) we find

$$\begin{aligned}
 g_{V_L} &= 0.07 - i 0.16, & g_{V_R} &= -0.01 - i 0.39, \\
 g_{S_L} &= -0.29 - i 0.67, & g_{S_R} &= 0.19 + i 0.08, & g_{T_L} &= 0.11 - i 0.18.
 \end{aligned}
 \tag{46}$$

In Fig. 2 we show the q^2 -dependence of each observable relevant to $\bar{B} \rightarrow D^* \tau \bar{\nu}$ discussed in the previous Section, both in the SM and with g_i given in Eq. (45).

After integrating over q^2 's as described in Eq. (43), and by sweeping over the entire range of g_i allowed by $R(D)^{\text{exp}}$ and $R(D^*)^{\text{exp}}$, we obtain the results listed in Tab. 2 and Tab. 3. The results are presented along with the SM ones in order to make a comparison simpler. Notice that the SM values we obtain are fully compatible with those quoted in Eq. (2), obtained by HFLAV, even though the central values are slightly different owing to

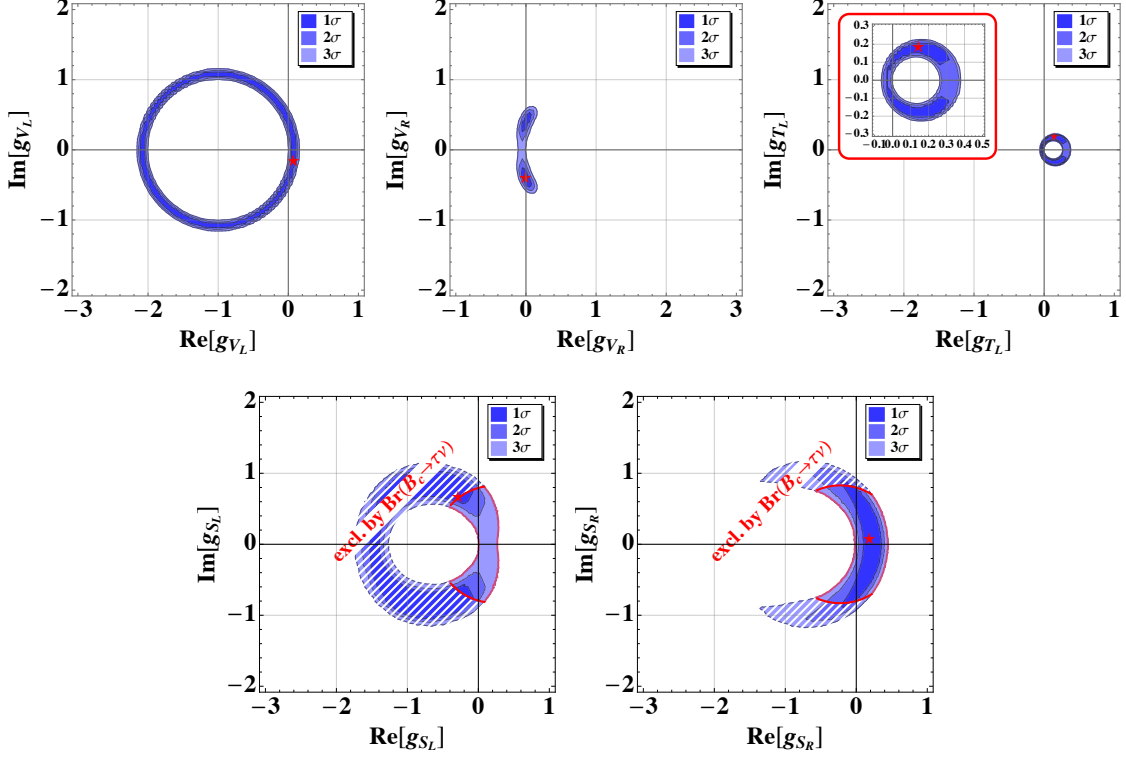


Figure 4: Same as in Fig. 3 but for the NP couplings appearing in Eq.(6).

our choice of form factors. For each g_i we then compute $R(D)$ and $R(D^*)$, which are now obviously compatible with experimental values, and the full list of the LFUV observables discussed in the previous Section. For the observables showing gaussian shapes we quote the mean values with the corresponding standard deviations. Some of the observables, however, are hardly gaussian for the reasons explained below. For such observables in Tabs. 2 and 3 we present the interval of values within 2σ . The interested reader can also find in the tables of Appendix E the predictions for all the LFUV observables obtained assuming for the benchmark values for the NP couplings given in Eqs. (45,46).

Let us now comment on the results we obtain, starting from the ones shown in Tab. 2.

- $\underline{g_V}$: Assuming NP affecting only the vector current, the constraints arising from $R(D)^{\text{exp}}$ and $R(D^*)^{\text{exp}}$ are such that either no or very small deviation of the LFUV observables with respect to their SM values is predicted. The only exception is $R(A_3)$ which, for allowed $g_V \neq 0$, becomes lower than its SM counterpart.

Notice that for several observables we give only the intervals due to their non-gaussian behaviour. They can be divided into two classes: those only sensitive to $\mathcal{R}e(g_V)$, such as $R(A_{FB}^{D^*})$, $R(A_5)$ and $R(A_6)$, and those only sensitive to $\mathcal{I}m(g_V)$, namely $D(A_7)$, $D(A_8)$ and $D(A_9)$. Let us focus on one observable from the first class, say $R(A_5)$. As stated above, its value would be indistinguishable from the SM for g_V purely

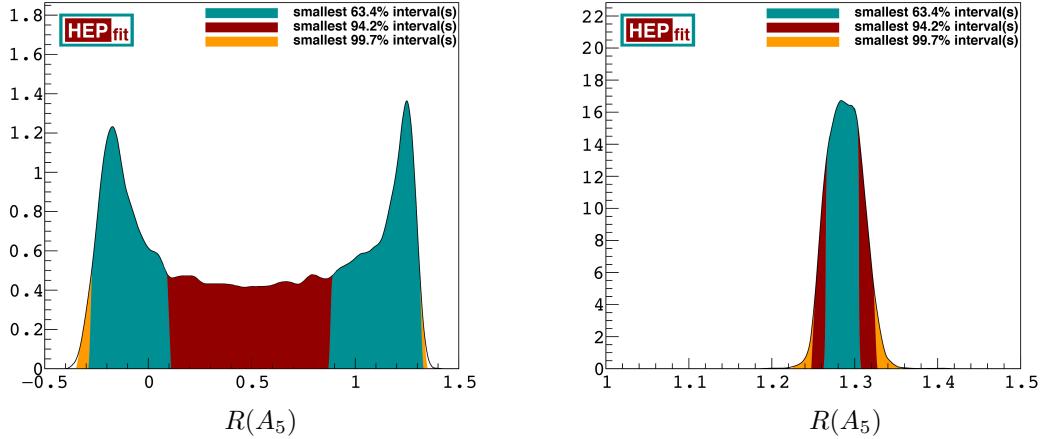


Figure 5: *Left panel: predicted p.d.f. for the observable $R(A_5)$, assuming a complex g_V . Right panel: predicted p.d.f. for the observable $R(A_5)$, assuming that g_V is equal to the best fit value reported in Eq. (45).*

imaginary. From the plot shown in the first panel of Fig. 3 it is apparent that there are 2 distinct allowed solutions for $\text{Re}(g_V)$ when $\text{Im}(g_V) = 0$, and therefore there are 2 distinct predictions of $R(A_5)$. After sweeping through various $\text{Im}(g_V)$ we fill up the gap between the two distinct real solutions in the case of $\text{Im}(g_V) = 0$, hence producing the anticipated non-gaussian prediction for $R(A_5)$, shown in the left panel of Fig. 5.

At first sight, given the broad range of predicted values, this observable might not seem of particular use. However, a careful reader will realize that a given value of g_V will correspond to a point (and not a disk) in the plane depicted in the first panel of Fig. 3. Therefore, for a given value of $\text{Re}(g_V)$, one gets a very sharp prediction for $R(A_5)$ as shown in the right panel of Fig. 5, where we assumed that g_V is equal to its best fit value reported in Eq. (45). Conversely, the measurement of $R(A_5)$ would produce a sharp bound on the real part of g_V , corresponding to a vertical stripe in the $\text{Re}(g_V)$ - $\text{Im}(g_V)$ plane that intersected with the disk produced by the measurements of $R(D)$ and $R(D^*)$, therefore severely reducing the allowed region for that coupling.

As stated above, a similar reasoning can be performed for $R(A_{FB}^{D*})$, $R(A_6)$, $D(A_7)$, $D(A_8)$ and $D(A_9)$, hence making all these observable extremely interesting.

- $\underline{g_A}$: If NP appears only in the axial current, only the $B \rightarrow D^* \tau \nu_\tau$ channel is affected. Similarly to the previous scenario the obtained bounds are such that no appreciable difference is observed in the observables $R(A_{\lambda_\ell}^{D*})$, $R(R_{L,T})$, $R(R_{A,B})$, $R(A_3)$ and $R(A_4)$. On the other hand, analogously to the g_V scenario, for $R(A_{FB}^{D*})$, $R(A_5)$, $R(A_6)$, $D(A_7)$, $D(A_8)$ and $D(A_9)$ we get broad ranges of values, with the LFUV

ratios affected by $Re(g_A)$ and the LFUV differences by $Im(g_A)$. Like in the vector scenario, the measurement of these observables would highly constrain the allowed region for g_A .

- $\underline{g_S}$: If the NP effects come with the contribution arising solely from the scalar operator, then only $B \rightarrow D\tau\nu_\tau$ would be affected. In particular, $R(A_{\chi_\ell}^D)$ is sensibly shifted compared to the SM prediction, while $R(A_{FB}^D)$ displays once again a broad prediction, due to its sensitivity to $Re(g_S)$. Therefore, its measurement would provide the strongest bound on g_S .
- $\underline{g_P}$: In contrast to the previous case, the NP giving a nonzero contribution to a term proportional to the pseudoscalar current would result in the changes in the $B \rightarrow D^*\tau\nu_\tau$ channel only. The unaffected observables by this choice would be $R(R_{A,B})$, $D(A_8)$ and $D(A_9)$. On the other hand, $R(A_{\chi_\ell}^{D*})$, $R(R_{L,T})$, $R(A_3)$, $R(A_4)$ and $R(A_6)$ are all predicted with good precision, and sensibly different from the values predicted in the SM. Moreover, we again obtain broad ranges for $R(A_{FB}^{D*})$, $R(A_5)$ and $D(A_7)$, with $Re(g_P)$ affecting the LFUV ratios, while $Im(g_P) \neq 0$ would particularly affect the LFUV differences.
- $\underline{g_T}$: If the NP effects give a nonzero contribution to the term proportional to the tensor current then both channels are affected. Furthermore, all the LFUV ratios are predicted with fairly good precision and with sensible discrepancies when compared with the SM predictions. Regarding the LFUV differences, $D(A_7)$ is the only one mildly affected by $g_T \neq 0$, even if perfectly compatible with the SM prediction, while the remaining ones are both unaffected by this kind of NP.

Similar observations can be obtained analyzing the results from Tab. 3, where we have not listed the results relative to g_{T_L} since they are the same as the ones obtained for g_T , owing to Eq.(7).

- $\underline{g_{V_L}}$: If the effects come with the left-handed vector current alone then the present experimental bounds are such that no sensible deviation can be appreciated in any of the LFUV quantities defined above.
- $\underline{g_{V_R}}$: In contrast to the previous case, if the coupling to the right-handed vector current is preferred then some LFUV observables in the $B \rightarrow D^*\tau\nu_\tau$ channel exhibit a sensitivity to its effects, namely $R(A_{FB}^{D*})$, $R(A_5)$, $R(A_6)$, $D(A_7)$, $D(A_8)$ and $D(A_9)$. Moreover, given that the LFUV differences depend on $Im(g_{V_R})$ and that, as can be observed from the second panel of Fig. 4, the fit allows for two distinct solutions for $Im(g_{V_R})$, we obtain two separate predicted regions for each of these observables. Notice that the range of allowed g_{V_R} is far more restricted by the data which is expected on the basis of the SM gauge invariance.

- g_{S_L} and g_{S_R} : Assuming NP effects in the scalar current, we obtain both in the left-handed and in the right-handed cases a similar outcome: three observables are unaffected, namely $R(R_{A,B})$, $D(A_8)$ and $D(A_9)$, while $R(A_{\lambda_\ell}^D)$ is found to be sensibly different with respect to its SM value. All the remaining observables display broad prediction ranges, once again with the real (imaginary) part affecting the LFUV ratios (differences).

To further explore the possibilities of using the angular observables as tests for LFUV we performed an extra test, motivated by the following observation: as can be seen from Eq. (23), only a small subset of the angular coefficients defined at Eq. (18) appear in the definition of the decay rate and hence of $R(D^*)$, i.e. $I_{1c,1s}$ and $I_{2c,2s}$. Therefore, the measurement of the branching fraction can constrain only a part of the coefficients appearing in the full angular distribution defined in Eq. (17), with the remaining ones still potentially affected by the NP effects. In order to test such effects we performed a new set of fits where we assumed that $R(D)$ and $R(D^*)$ would be measured with a central value equal to the SM predictions with a 10% error. The allowed regions for the couplings are found to be similar to the ones shown in Figs. 3 and 4, even if reduced in size and thickness. Therefore, the LFUV observables that were previously showing a broad prediction due to their non-trivial interplay with the real and the imaginary parts of the NP couplings will continue to display such a behavior. In other words, even if $R(D)$ and $R(D^*)$ are measured to agree with the SM predictions, there are 7 angular observables that might still display a behavior unambiguously related to NP effects: four LFUV ratios [$R(A_{FB}^{D,D^*})$, $R(A_{5,6})$], and three LFUV differences [$D(A_{7,8,9})$].

All of the above observations show the impact that the measurement of even a small subset of the observables presented in Sec. 2.4 would have on our understanding of the NP contribution to the $b \rightarrow c$ transitions. In particular, the measurement of any of the observables between $R(A_{FB}^{D,D^*})$, $R(A_{5,6})$ and $D(A_{7,8,9})$ would be of great interest, given their twofold power: they would help deciphering the Lorentz structure of the NP contributions, and they would severely constrain the presently allowed region for the NP couplings. We emphasize once again that a measurement of these observables would be of great interest even in the case of $R(D)$ and $R(D^*)$ being fully compatible with their SM values.

3.2 Comment of $F_L^{D^*}$

Very recently the Belle Collaboration presented the results of their first study of the fraction of the longitudinally polarized D^* 's in their full sample of $B \rightarrow D^{(*)}\tau\bar{\nu}$ and found $F_L^{D^*} = 0.60(9)$ [72], where we combined the experimental errors in quadrature. That value turns out to be less than 2σ larger than predicted in the SM, which we find to be $(F_L^{D^*})^{\text{SM}} = 0.47(2)$. As it can be seen in the last line of Tabs. 2 and 3, it is very difficult to make the value of $F_L^{D^*} > (F_L^{D^*})^{\text{SM}}$. Only a marginal enhancement is allowed by switching on $g_{S_L, S_R, P}$ while all the other non-zero NP coefficients would make $F_L^{D^*} < (F_L^{D^*})^{\text{SM}}$. We hope

this quantity will be further scrutinized by the other experimental groups and its precision will be improved to the point that it can play an important role in discriminating among various models.

Since we consistently assume that NP arises from coupling to τ , measuring this quantity in the case of μ or e in the final state would be a very helpful check of our assumption. In other words, if our assumption is right then the measured $F_L^{D^*}(\mu, e)$ should be equal to $(F_L^{D^*}(\mu, e))^{\text{SM}} = 0.52(1)$.

4 Summary

In this paper we discussed a possibility of using a set of observables that can be extracted from the angular distribution of the $B \rightarrow D^{(*)}l\bar{\nu}$ decays in order to study the effects of LFUV. In particular, we define 3 such observables that can be obtained from the angular distribution of the $B \rightarrow D\ell\bar{\nu}$ decay, and 12 from $B \rightarrow D^*\ell\bar{\nu}$.

NP contribution to $B \rightarrow D^{(*)}\tau\bar{\nu}$ can be parametrized by the couplings $g_{V_L, V_R, S_L, S_R, T_L}$ (defined in the text), the values of which can be constrained by the experimentally measured $R(D^{(*)})$, found to be larger than its SM prediction. We explored the possibility of feeding $R(D^{(*)})^{\text{exp}} - R(D^{(*)})^{\text{SM}}$ by turning on one coupling at the time and found that the measurement even of a subset of observables can indeed help disentangling among various possibilities. In other words, their measurement can considerably help in constraining the complex valued couplings g_i 's and thereby help us understanding the Lorentz structure of the NP contribution(s). For that purpose, like in the case of $R(D^{(*)})$ we point out that for the observables for which the SM prediction is non-zero it is convenient to consider the ratios between the value extracted from the $B \rightarrow D^{(*)}\tau\bar{\nu}$ mode and the one extracted from $B \rightarrow D^{(*)}l\bar{\nu}$ with $l \in (e, \mu)$. Instead, for the quantities which are zero in the SM we consider the differences.

Since many of the proposed observables provide information of the NP couplings that cannot be accessed through the measurement of the branching fraction, we show that even in the case in which $R(D^{(*)})^{\text{exp}} = R(D^{(*)})^{\text{SM}}$ one can still have non-zero NP couplings which can be checked by measuring the ratios/differences of the observables deduced from the angular distributions of the considered decay modes.

Even though the observables discussed in this paper are most interesting in the case of τ -lepton in the final state, their experimental measurements in the case of e and/or μ in the final state are very important too. They would help us checking on the assumption that is mostly made in the literature, namely that the NP affects only the couplings to τ and not to e or μ . In that case the measurements would coincide with the SM predictions.

Furthermore, in some models of NP the coupling to μ can be large whereas the one to the electron negligibly small [73]. In that situation it is very important to check also on the ratios of the observables discussed here in the case of $B \rightarrow D^{(*)}\mu\bar{\nu}$ with respect to those measured in the case of $B \rightarrow D^{(*)}e\bar{\nu}$.

Finally, in order to make this study quantitatively sound, beside the experimental input, one also needs the lattice QCD information concerning the shapes of hadronic form factors relevant to the $B \rightarrow D^* \ell \bar{\nu}$ decay, which are still missing.

Acknowledgements

We wish to thank Gudrun Hiller and Donal Hill for useful discussions during the completion of the manuscript. M.F. thanks the Fondazione Della Riccia for partial financial support during the completion of this work, and acknowledges the financial support from MINECO grant FPA2016-76005-C2-1-P, Maria de Maetzu program grant MDM-2014-0367 of ICCUB and 2017 SGR 929. The work of I.N. is supported by BMBF under grant no. 05H18VKKB1. The work of A.T. has been supported by the DFG Research Unit FOR 1873 “Quark Flavour Physics and Effective Field Theories”. This project has also received support from the European Union’s Horizon 2020 research and innovation programme under the Marie Skłodowska-Curie grant agreement N. 690575 and 674896.

Obs.	Exp.	SM	g_V	g_A	g_S	g_P	g_T
R_D	0.334 ± 0.029	0.30 ± 0.02	0.37 ± 0.03	—	0.37 ± 0.03	—	0.34 ± 0.03
R_{D^*}	0.297 ± 0.015	0.258 ± 0.003	0.261 ± 0.003	0.30 ± 0.01	—	0.278 ± 0.007	0.30 ± 0.01
$R(A_{FB}^D)$	—	0.077 ± 0.004	0.074 ± 0.003	—	$[-0.058, 0.074]$	—	0.082 ± 0.004
$R(A_{\chi_\ell}^D)$	—	-0.332 ± 0.003	-0.331 ± 0.003	—	-0.48 ± 0.05	—	-0.25 ± 0.05
$R(A_{\chi_\ell}^{D^*})$	—	0.47 ± 0.02	0.48 ± 0.04	0.48 ± 0.02	—	0.36 ± 0.04	0.18 ± 0.14
$R(R_{L,T})$	—	0.79 ± 0.02	0.78 ± 0.02	0.80 ± 0.02	—	0.95 ± 0.05	0.42 ± 0.14
$R(R_{A,B})$	—	0.520 ± 0.004	0.514 ± 0.005	0.524 ± 0.004	—	0.516 ± 0.004	0.64 ± 0.07
$R(A_{FB}^{D^*})$	—	0.23 ± 0.04	$[-1.52, 0.40]$	$[-1.38, 0.20]$	—	0.00 ± 0.06	-0.02 ± 0.06
$R(A_3)$	—	0.62 ± 0.01	0.58 ± 0.01	0.63 ± 0.02	—	0.56 ± 0.02	0.11 ± 0.23
$R(A_4)$	—	0.46 ± 0.01	0.45 ± 0.01	0.46 ± 0.01	—	0.42 ± 0.01	0.06 ± 0.18
$R(A_5)$	—	1.15 ± 0.02	$[-0.26, 1.28]$	$[-0.09, 1.12]$	—	1.24 ± 0.05	0.42 ± 0.30
$R(A_6)$	—	0.79 ± 0.01	$[-0.96, 0.96]$	$[-0.76, 0.76]$	—	0.72 ± 0.02	0.15 ± 0.25
$D(A_7)$	—	0	$[-0.05, 0.05]$	$[-0.04, 0.04]$	—	0.00 ± 0.01	0.00 ± 0.02
$D(A_8)$	—	0	$[-0.03, 0.03]$	$[-0.03, 0.03]$	—	0	0
$D(A_9)$	—	0	$[-0.09, 0.09]$	$[-0.07, 0.07]$	—	0	0
$F_L^{D^*}$	—	0.47 ± 0.02	0.46 ± 0.02	0.46 ± 0.02	—	0.51 ± 0.02	0.32 ± 0.13

Table 2: The values of LFUV ratios/differences. Besides the SM results in each following column we show the results obtained by switching on the NP coupling g_i [$i \in \{V, A, S, P, T\}$] corresponding to that column in such a way that we sweep through the values allowed by $R(D^{(*)\text{exp}}$ as shown in Fig. 3. For the quantities which barely exhibit a gaussian behavior (for the reasons discussed in the text) we provide the 2σ ranges. In the last line we also give the corresponding value of the fraction of longitudinally polarized D^* in the sample of $B \rightarrow D^{(*)}\tau\bar{\nu}$.

Obs.	Exp.	SM	g_{V_L}	g_{V_R}	g_{S_L}	g_{S_R}
R_D	0.334 ± 0.029	0.30 ± 0.02	0.33 ± 0.02	0.33 ± 0.03	0.36 ± 0.03	0.36 ± 0.03
R_{D^*}	0.297 ± 0.014	0.258 ± 0.003	0.30 ± 0.01	0.30 ± 0.01	0.26 ± 0.01	0.259 ± 0.005
$R(A_{FB}^D)$	—	0.077 ± 0.004	0.074 ± 0.003	0.074 ± 0.003	0.06 ± 0.01	0.06 ± 0.01
$R(A_{\lambda_e}^D)$	—	-0.332 ± 0.003	-0.331 ± 0.003	-0.331 ± 0.003	-0.47 ± 0.05	-0.47 ± 0.05
$R(A_{X_e}^{D^*})$	—	0.47 ± 0.02	0.48 ± 0.02	0.49 ± 0.02	0.47 ± 0.05	0.46 ± 0.03
$R(R_{L,T})$	—	0.79 ± 0.02	0.79 ± 0.02	0.79 ± 0.02	0.81 ± 0.05	0.82 ± 0.03
$R(R_{A,B})$	—	0.520 ± 0.004	0.520 ± 0.004	0.520 ± 0.005	0.520 ± 0.004	0.520 ± 0.004
$R(A_{FB}^{D^*})$	—	0.23 ± 0.04	0.23 ± 0.04	-0.01 ± 0.05	0.24 ± 0.08	0.23 ± 0.08
$R(A_3)$	—	0.62 ± 0.01	0.62 ± 0.02	0.61 ± 0.03	0.61 ± 0.02	0.61 ± 0.01
$R(A_4)$	—	0.46 ± 0.01	0.46 ± 0.01	0.46 ± 0.01	0.46 ± 0.01	0.45 ± 0.01
$R(A_5)$	—	1.15 ± 0.02	1.15 ± 0.03	0.97 ± 0.05	1.04 ± 0.03	1.12 ± 0.06
$R(A_6)$	—	0.79 ± 0.01	0.80 ± 0.02	0.55 ± 0.05	0.79 ± 0.02	0.78 ± 0.02
$D(A_7)$	—	0	0	-0.028 ± 0.005 0.028 ± 0.005	$[-0.02, 0.02]$	$[-0.02, 0.02]$
$D(A_8)$	—	0	0	-0.019 ± 0.003 0.019 ± 0.003	0	0
$D(A_9)$	—	0	0	-0.05 ± 0.01 0.05 ± 0.01	0	0
F_{D^*}	—	0.47 ± 0.02	0.46 ± 0.02	0.46 ± 0.02	0.47 ± 0.05	0.47 ± 0.04

Table 3: Same as in Tab. 2 but in the basis defined in the effective Hamiltonian (6). We stress that for the form factors we use CLN+HQET+LATT, as discussed in the text.

A Form factors

The hadronic matrix element are parametrized as follows:

$$\langle D(k)|\bar{c}\gamma_\mu b|\bar{B}(p)\rangle = \left[(p+k)_\mu - \frac{m_B^2 - m_D^2}{q^2} q_\mu \right] f_+(q^2) + q_\mu \frac{m_B^2 - m_D^2}{q^2} f_0(q^2), \quad (47)$$

$$\begin{aligned} \langle D(k)|\bar{c}b|\bar{B}(p)\rangle &= \frac{1}{m_b - m_c} q^\mu \langle D(k)|\bar{c}\gamma_\mu b|\bar{B}(p)\rangle = \frac{m_B^2 - m_D^2}{m_b - m_c} f_0(q^2), \\ \langle D(k)|\bar{c}\gamma_5 b|\bar{B}(p)\rangle &= 0, \end{aligned} \quad (48)$$

$$\begin{aligned} \langle D(k)|\bar{c}\sigma_{\mu\nu} b|\bar{B}(p)\rangle &= -i(p_\mu k_\nu - k_\mu p_\nu) \frac{2f_T(q^2)}{m_B + m_D}, \\ \langle D(k)|\bar{c}\sigma_{\mu\nu}\gamma_5 b|\bar{B}(p)\rangle &= -\frac{i}{2}\epsilon_{\mu\nu\alpha\beta}\langle D(k)|\bar{c}\sigma^{\alpha\beta} b|\bar{B}(p)\rangle = -\epsilon_{\mu\nu\alpha\beta} p^\alpha k^\beta \frac{2f_T(q^2)}{m_B + m_D}. \end{aligned} \quad (49)$$

$$\begin{aligned} \langle D^*(k, \varepsilon)|\bar{c}\gamma_\mu b|\bar{B}(p)\rangle &= -i\epsilon_{\mu\nu\alpha\beta}\varepsilon^{*\nu} p^\alpha k^\beta \frac{2V(q^2)}{m_B + m_{D^*}}, \\ \langle D^*(k, \varepsilon)|\bar{c}\gamma_\mu\gamma_5 b|\bar{B}(p)\rangle &= \varepsilon_\mu^*(m_B + m_{D^*})A_1(q^2) - (p+k)_\mu(\varepsilon^*q) \frac{A_2(q^2)}{m_B + m_{D^*}} \\ &\quad - q_\mu(\varepsilon^*q) \frac{2m_{D^*}}{q^2} [A_3(q^2) - A_0(q^2)], \end{aligned} \quad (50)$$

with

$$A_3(q^2) = \frac{m_B + m_{D^*}}{2m_{D^*}} A_1(q^2) - \frac{m_B - m_{D^*}}{2m_{D^*}} A_2(q^2), \quad (51)$$

$$\begin{aligned} \langle D^*(k, \varepsilon)|\bar{c}b|\bar{B}(p)\rangle &= 0, \\ \langle D^*(k, \varepsilon)|\bar{c}\gamma_5 b|\bar{B}(p)\rangle &= -\frac{1}{m_b + m_c} q^\mu \langle D^*(k, \varepsilon)|\bar{c}\gamma_\mu\gamma_5 b|\bar{B}(p)\rangle \\ &= -(\varepsilon^*q) \frac{2m_{D^*}}{m_b + m_c} A_0(q^2), \end{aligned} \quad (52)$$

The tensor contribution can be parametrized as

$$\begin{aligned} \langle D^*(k, \varepsilon)|\bar{c}\sigma_{\mu\nu} b|\bar{B}(p)\rangle &= \epsilon_{\mu\nu\alpha\beta} [\varepsilon^{*\alpha}(p+k)^\beta g_+(q^2) + \varepsilon^{*\alpha} q^\beta g_-(q^2) \\ &\quad + (\varepsilon^*q) p^\alpha k^\beta g_0(q^2)], \\ \langle D^*(k, \varepsilon)|\bar{c}\sigma_{\mu\nu}\gamma_5 b|\bar{B}(p)\rangle &= -\frac{i}{2}\epsilon_{\mu\nu\alpha\beta}\langle D^*(k, \varepsilon)|\bar{c}\sigma^{\alpha\beta} b|\bar{B}(p)\rangle \\ &= i \left\{ [\varepsilon_\mu^*(p+k)_\nu - (p+k)_\mu \varepsilon_\nu^*] g_+(q^2) \right. \\ &\quad \left. + [\varepsilon_\mu^* q_\nu - q_\mu \varepsilon_\nu^*] g_-(q^2) + (\varepsilon^*q) [p_\mu k_\nu - k_\mu p_\nu] g_0(q^2) \right\}, \end{aligned} \quad (53)$$

where $g_{\pm,0}$ can be related to the ‘‘standard’’ T_{1-3} form factors as

$$\begin{aligned} g_+(q^2) &= -T_1(q^2), \\ g_-(q^2) &= \frac{m_B^2 - m_{D^*}^2}{q^2} [T_1(q^2) - T_2(q^2)], \\ g_0(q^2) &= \frac{2}{q^2} \left[T_1(q^2) - T_2(q^2) - \frac{q^2}{m_B^2 - m_{D^*}^2} T_3(q^2) \right]. \end{aligned} \quad (54)$$

The additional form factors commonly used in the literature are defined as

$$\begin{aligned} A_{12}(q^2) &= \frac{1}{16m_B m_{D^*}^2} \left[(m_B^2 - m_{D^*}^2 - q^2)(m_B + m_{D^*})A_1(q^2) - \frac{\lambda_{BD^*}(q^2)}{m_B + m_{D^*}} A_2(q^2) \right], \\ T_{23}(q^2) &= \frac{1}{8m_B m_{D^*}^2} \left[(m_B^2 + 3m_{D^*}^2 - q^2)(m_B + m_{D^*})T_2(q^2) - \frac{\lambda_{BD^*}(q^2)}{m_B - m_{D^*}} T_3(q^2) \right]. \end{aligned} \quad (55)$$

In order to cancel the divergence at $q^2 = 0$, the following conditions must be imposed

$$f_+(0) = f_0(0), \quad A_0(0) = A_3(0), \quad T_1(0) = T_2(0), \quad A_{12}(0) = \frac{m_B^2 - m_{D^*}^2}{8m_B m_{D^*}} A_3(0). \quad (56)$$

In this work we use the convention $\epsilon_{0123} = 1$ (or equivalently $\epsilon^{0123} = -1$). Note that for the alternative convention, $\epsilon_{0123} = -1$, the pseudo-tensor matrix elements in Eqs.(49),(53) change the sign since $\sigma_{\mu\nu}\gamma_5 = -\text{sgn}[\epsilon_{0123}](i/2)\epsilon_{\mu\nu\alpha\beta}\sigma^{\alpha\beta}$.

B Helicity amplitude formalism

Using the property of the off-shell vector boson V^* polarization vectors,

$$\sum_{\lambda} \eta_{\mu}^*(\lambda)\eta_{\nu}(\lambda)\delta_{\lambda} = g_{\mu\nu}, \quad \delta_{0,\pm} = -\delta_t = -1, \quad (57)$$

one can write the $\bar{B} \rightarrow MV^* \rightarrow M\ell\bar{\nu}$ ($M = D, D^*$) amplitudes of general vector and tensor currents as

$$\begin{aligned} \mathcal{M}_{V(A)}^{\lambda_M, \lambda_{\ell}} &\propto \langle M(\lambda_M) | J_{\text{had}}^{\mu} | \bar{B} \rangle \langle \ell(\lambda_{\ell}) \bar{\nu} | J_{\text{lep}, \mu} | 0 \rangle \\ &= \sum_{\lambda} \eta_{\mu}^*(\lambda) \langle M(\lambda_M) | J_{\text{had}}^{\mu} | \bar{B} \rangle \eta_{\nu}(\lambda) \langle \ell(\lambda_{\ell}) \bar{\nu} | J_{\text{lep}, \nu}^{\nu} | 0 \rangle \delta_{\lambda} \\ &= \sum_{\lambda} \delta_{\lambda} H_{V(A), \lambda}^{\lambda_M} L_{V-A, \lambda}^{\lambda_{\ell}}, \\ \mathcal{M}_{T(T5)}^{\lambda_M, \lambda_{\ell}} &\propto \langle M(\lambda_M) | J_{\text{had}}^{\mu\nu} | \bar{B} \rangle \langle \ell(\lambda_{\ell}) \bar{\nu} | J_{\text{lep}, \mu\nu} | 0 \rangle \\ &= \sum_{\lambda, \lambda'} i \eta_{\mu}^*(\lambda) \eta_{\nu}^*(\lambda') \langle M(\lambda_M) | J_{\text{had}}^{\mu\nu} | \bar{B} \rangle (-i) \eta_{\alpha}(\lambda) \eta_{\beta}(\lambda') \langle \ell(\lambda_{\ell}) \bar{\nu} | J_{\text{lep}}^{\alpha\beta} | 0 \rangle \delta_{\lambda} \delta_{\lambda'} \\ &= \sum_{\lambda, \lambda'} \delta_{\lambda} \delta_{\lambda'} H_{T(T5), \lambda\lambda'}^{\lambda_M} L_{T-T5, \lambda\lambda'}^{\lambda_{\ell}}, \end{aligned} \quad (58)$$

where H and L denote the leptonic and hadronic helicity amplitudes defined in Eqs. (63),(67). The $\pm i$ factors in $\mathcal{M}_{T(T5)}$ are introduced for convenience, in order to make all hadronic $\bar{B} \rightarrow MV^*$ and leptonic amplitudes real if $g_i \in \mathbb{R}$ and when $\chi \rightarrow 0$ (cf. Fig. 1). The scalar amplitude is simply defined as

$$\mathcal{M}_{S(P)}^{\lambda_\ell} \propto \langle M(\lambda_M = 0) | J_{\text{had}} | \bar{B} \rangle \langle \ell(\lambda_\ell) \bar{\nu} | J_{\text{lep}} | 0 \rangle = H_{S(P)} L_{S-P}^{\lambda_\ell}. \quad (59)$$

Here λ_M and $\lambda^{(\prime)}$ denote the meson and the virtual boson helicities in the \bar{B} reference frame. The lepton helicity λ_ℓ is defined in the $\ell\bar{\nu}$ rest frame.

For the four-body final state $\bar{B} \rightarrow D^*V^* \rightarrow D\pi\ell\bar{\nu}$ decay the total amplitude has the form

$$\mathcal{M}_X^{\lambda_M, \lambda_\ell} \propto \langle D\pi | D^*(\lambda_{D^*}) \rangle \langle D^*(\lambda_{D^*}) | J_{\text{had}}^X | \bar{B} \rangle \langle \ell(\lambda_\ell) \bar{\nu} | J_{\text{lep}, X} | 0 \rangle BW_{D^*}, \quad (60)$$

where the propagation of the intermediate resonant state is parametrized by the Breit-Wigner function,

$$BW_{D^*}(m_{D\pi}^2) = \frac{1}{m_{D\pi}^2 - m_{D^*}^2 + im_{D^*}\Gamma_{D^*}}. \quad (61)$$

Since the width of D^* is very small, one can use the narrow width approximation,

$$\frac{1}{(m_{D\pi}^2 - m_{D^*}^2)^2 + m_{D^*}^2\Gamma_{D^*}^2} \xrightarrow{\Gamma_{D^*} \ll m_{D^*}} \frac{\pi}{m_{D^*}\Gamma_{D^*}} \delta(m_{D\pi}^2 - m_{D^*}^2), \quad (62)$$

and integrate out the $m_{D\pi}$ dependence in the phase space.

B.1 Leptonic amplitudes

The leptonic amplitudes are defined as

$$\begin{aligned} L_{V-A, \lambda}^{\lambda_\ell}(q^2, \chi, \theta_\ell) &= \eta_\mu(\lambda) \langle \ell(\lambda_\ell) \bar{\nu} | \bar{\ell} \gamma^\mu (1 - \gamma_5) \nu | 0 \rangle, \\ L_{S-P}^{\lambda_\ell}(q^2, \chi, \theta_\ell) &= \langle \ell(\lambda_\ell) \bar{\nu} | \bar{\ell} (1 - \gamma_5) \nu | 0 \rangle, \\ L_{T-T5, \lambda\lambda'}^{\lambda_\ell}(q^2, \chi, \theta_\ell) &= -L_{T-T5, \lambda'\lambda}^{\lambda_\ell} = -i\eta_\mu(\lambda)\eta_\nu(\lambda') \langle \ell(\lambda_\ell) \bar{\nu} | \bar{\ell} \sigma^{\mu\nu} (1 - \gamma_5) \nu | 0 \rangle. \end{aligned} \quad (63)$$

Using the polarization vectors and Dirac spinors, given in the Appendix C, and gamma-matrices in the Weyl (chiral) representation, one can obtain the explicit formulas for the vector type amplitudes:

$$\begin{aligned} L_{V-A, +}^+(q^2, \chi, \theta_\ell) &= \pm\sqrt{2}m_\ell\beta_\ell \sin\theta_\ell e^{-2i\chi}, \\ L_{V-A, -}^+(q^2, \chi, \theta_\ell) &= \pm\sqrt{2}m_\ell\beta_\ell \sin\theta_\ell, \\ L_{V-A, 0}^+(q^2, \chi, \theta_\ell) &= 2m_\ell\beta_\ell \cos\theta_\ell e^{-i\chi}, \\ L_{V-A, t}^+(q^2, \chi, \theta_\ell) &= -2m_\ell\beta_\ell e^{-i\chi}, \\ L_{V-A, \pm}^-(q^2, \chi, \theta_\ell) &= \sqrt{2q^2}\beta_\ell(1 \pm \cos\theta_\ell) e^{\mp i\chi}, \\ L_{V-A, 0}^-(q^2, \chi, \theta_\ell) &= -2\sqrt{q^2}\beta_\ell \sin\theta_\ell, \\ L_{V-A, t}^-(q^2, \chi, \theta_\ell) &= 0, \end{aligned} \quad (64)$$

with $\beta_\ell = \sqrt{1 - m_\ell^2/q^2}$. Expressions for the scalar leptonic amplitudes read

$$\begin{aligned} L_{S-P}^+(q^2, \chi, \theta_\ell) &= -2\sqrt{q^2}\beta_\ell e^{-i\chi}, \\ L_{S-P}^-(q^2, \chi, \theta_\ell) &= 0. \end{aligned} \quad (65)$$

Finally, the tensor type amplitudes are given by

$$\begin{aligned} L_{T-T5,+0}^+(q^2, \chi, \theta_\ell) &= \sqrt{2q^2}\beta_\ell \sin\theta_\ell e^{-2i\chi}, \\ L_{T-T5,-0}^+(q^2, \chi, \theta_\ell) &= \sqrt{2q^2}\beta_\ell \sin\theta_\ell, \\ L_{T-T5,+-}^+(q^2, \chi, \theta_\ell) &= -L_{T-T5,0t}^+ = 2\sqrt{q^2}\beta_\ell \cos\theta_\ell e^{-i\chi}, \\ L_{T-T5,++}^+(q^2, \chi, \theta_\ell) &= \mp\sqrt{2q^2}\beta_\ell \sin\theta_\ell e^{-2i\chi}, \\ L_{T-T5,-t}^+(q^2, \chi, \theta_\ell) &= \mp\sqrt{2q^2}\beta_\ell \sin\theta_\ell, \\ L_{T-T5,\pm 0}^-(q^2, \chi, \theta_\ell) &= \pm\sqrt{2}m_\ell\beta_\ell(1 \pm \cos\theta_\ell) e^{\mp i\chi}, \\ L_{T-T5,+-}^-(q^2, \chi, \theta_\ell) &= -L_{T-T5,0t}^- = -2m_\ell\beta_\ell \sin\theta_\ell, \\ L_{T-T5,\pm t}^-(q^2, \chi, \theta_\ell) &= -\sqrt{2}m_\ell\beta_\ell(1 \pm \cos\theta_\ell) e^{\mp i\chi}. \end{aligned} \quad (66)$$

By setting $\chi \rightarrow 0$ (i.e. the $x - z$ plane is defined by the lepton momentum) one ends up with the expressions coinciding with those given in Refs. [41, 74].

B.2 Hadronic amplitudes

The general helicity amplitudes, in the operator basis (5), read:

$$\begin{aligned} H_{V(A),\lambda}^{\lambda_M}(q^2) &= (g_{V(A)} \pm 1) \eta_\mu^*(\lambda) \langle M(\lambda_M) | \bar{c} \gamma^\mu (\gamma_5) b | \bar{B} \rangle, \\ H_{S(P),\lambda}(q^2) &= g_{S(P)} \langle M(\lambda_M = 0) | \bar{c} (\gamma_5) b | \bar{B} \rangle, \\ H_{T(T5),\lambda\lambda'}^{\lambda_M}(q^2) &= -H_{T,\lambda\lambda'}^{\lambda_M}(q^2) = i g_{T(T5)} \eta_\mu^*(\lambda) \eta_\nu^*(\lambda') \langle M(\lambda_M) | \bar{c} \sigma^{\mu\nu} (\gamma_5) b | \bar{B} \rangle, \end{aligned} \quad (67)$$

which can be written explicitly for the $\bar{B} \rightarrow D$ case as ⁴

$$h_0(q^2) \equiv h_{V,0}(q^2) = (g_V + 1) \sqrt{\frac{\lambda_{BD}(q^2)}{q^2}} f_+(q^2), \quad (68a)$$

$$h_t(q^2) \equiv h_{V,t}(q^2) = (g_V + 1) \frac{m_B^2 - m_D^2}{\sqrt{q^2}} f_0(q^2), \quad (68b)$$

$$h_S(q^2) \simeq g_S \frac{m_B^2 - m_D^2}{m_b - m_c} f_0(q^2), \quad (68c)$$

⁴To avoid confusion and simplify notation, we denote the $\bar{B} \rightarrow D$ amplitudes by h and omit the super-index $\lambda_D = 0$.

$$h_{T,0t}(q^2) = -\frac{g_T}{g_{T5}} h_{T5,+}(q^2) = -g_T \frac{\sqrt{\lambda_{BD}(q^2)}}{m_B + m_D} f_T(q^2), \quad (68d)$$

$$h_{A,\lambda}(q^2) = h_P(q^2) = h_{T,+}(q^2) = h_{T5,0t}(q^2) = 0, \quad (68e)$$

and for the $\bar{B} \rightarrow D^*$ case as

$$H_{V,\pm}^\pm(q^2) = \mp(g_V + 1) \frac{\sqrt{\lambda_{BD^*}(q^2)}}{m_B + m_{D^*}} V(q^2), \quad (69a)$$

$$H_{A,\pm}^\pm(q^2) = -(g_A - 1)(m_B + m_{D^*}) A_1(q^2), \quad (69b)$$

$$H_0(q^2) \equiv H_{A,0}^0(q^2) = (g_A - 1) \frac{8m_B m_{D^*}}{\sqrt{q^2}} A_{12}(q^2), \quad (69c)$$

$$H_t(q^2) \equiv H_{A,t}^0(q^2) = (g_A - 1) \sqrt{\frac{\lambda_{BD^*}(q^2)}{q^2}} A_0(q^2), \quad (69d)$$

$$H_P(q^2) \simeq -g_P \frac{\sqrt{\lambda_{BD^*}(q^2)}}{m_b + m_c} A_0(q^2), \quad (69e)$$

$$H_{T,\pm 0}^\pm(q^2) = \mp \frac{g_T}{g_{T5}} H_{T5,\pm t}^\pm(q^2) = \pm g_T \frac{m_B^2 - m_{D^*}^2}{\sqrt{q^2}} T_2(q^2), \quad (69f)$$

$$H_{T,\pm t}^\pm(q^2) = \mp \frac{g_T}{g_{T5}} H_{T5,\pm 0}^\pm(q^2) = \pm g_T \sqrt{\frac{\lambda_{BD^*}(q^2)}{q^2}} T_1(q^2), \quad (69g)$$

$$H_{T,+}^0(q^2) = -\frac{g_T}{g_{T5}} H_{T5,0t}^0(q^2) = -g_T \frac{4m_B m_{D^*}}{m_B + m_{D^*}} T_{23}(q^2), \quad (69h)$$

$$H_{V,0}^0(q^2) = H_{V,t}^0(q^2) = H_S(q^2) = H_{T,0t}^0(q^2) = H_{T5,+}^0(q^2) = 0, \quad (69i)$$

where again $\lambda_{BM}(q^2) = m_B^4 + m_M^4 + q^4 - 2(m_B^2 m_M^2 + m_B^2 q^2 + m_M^2 q^2)$. In deriving the expressions for the above amplitudes we used the decomposition of the hadronic matrix elements in terms of form factors listed in Appendix A.

B.3 $D^* \rightarrow D\pi$ amplitude

The $D^* \rightarrow D\pi$ amplitude can be parametrized as

$$\langle D\pi|D^*(\lambda_{D^*})\rangle = g_{D^*D\pi} \varepsilon_\mu(\lambda_{D^*}) p_D^\mu, \quad (70)$$

where the coupling $g_{D^*D\pi}$ parameterizes the physical $D^* \rightarrow D\pi$ decay and can be determined from the numerical simulations of QCD on the lattice or extracted from the measured width of D^{*+} ,

$$\Gamma(D^* \rightarrow D\pi) = \frac{C}{24\pi m_{D^*}^2} g_{D^*D\pi}^2 |\hat{\mathbf{p}}_D|^3, \quad (71)$$

where $C = 1$ if the outgoing pion is charged, and $C = 1/2$ if it is neutral, and $\hat{\mathbf{p}}_D$ is the D three-momentum in the D^* rest frame. It must be stressed that $g_{D^*D\pi}$ is $m_{D\pi}^2$ -independent, and the entire dependence of the amplitude (60) on $m_{D\pi}^2$ is assumed to be described by the Breit-Wigner function.

The amplitudes are computed in the D^* reference frame, where the D, π momenta are in the $x - z$ plane, and are given by

$$\begin{aligned} \langle D\pi|D^*(\pm 1)\rangle &= \pm \frac{1}{\sqrt{2}} g_{D^*D\pi} |\hat{\mathbf{p}}_D| \sin \theta_D, \\ \langle D\pi|D^*(0)\rangle &= -g_{D^*D\pi} |\hat{\mathbf{p}}_D| \cos \theta_D. \end{aligned} \quad (72)$$

B.4 Relations between amplitudes

One can notice from Eqs. (64) and (65) that

$$L_{S-P}^{\lambda_\ell} = \frac{\sqrt{q^2}}{m_\ell} L_{V-A,t}^{\lambda_\ell}. \quad (73)$$

Therefore, in order to further simplify the expressions, one can absorb the hadronic S/P amplitudes into the V/A time-like ones and redefine,

$$\tilde{H}_{V/A,t}^{\lambda_M(=0)} \equiv H_{V/A,t}^0 + \frac{\sqrt{q^2}}{m_\ell} H_{S/P}. \quad (74)$$

Moreover, from Eqs. (64) and (66) it can be seen that

$$\begin{aligned}
L_{T-T5, \pm 0}^+ &= \pm \frac{\sqrt{q^2}}{m_\ell} L_{V-A, \pm}^+, \\
L_{T-T5, +-}^+ &= -L_{T-T5, 0t}^+ = \frac{\sqrt{q^2}}{m_\ell} L_{V-A, 0}^+, \\
L_{T-T5, \pm t}^+ &= -\frac{\sqrt{q^2}}{m_\ell} L_{V-A, \pm}^+, \\
L_{T-T5, \pm 0}^- &= \pm \frac{m_\ell}{\sqrt{q^2}} L_{V-A, \pm}^-, \\
L_{T-T5, +-}^- &= -L_{T-T5, 0t}^- = \frac{m_\ell}{\sqrt{q^2}} L_{V-A, 0}^-, \\
L_{T-T5, \pm t}^- &= -\frac{m_\ell}{\sqrt{q^2}} L_{V-A, \pm}^-.
\end{aligned} \tag{75}$$

In this way, summing over the off-shell boson polarizations λ, λ' and taking into account the δ_λ factors in Eq. (58), one can write the general total amplitude as

$$\begin{aligned}
\mathcal{M}^{\lambda_M, \lambda_\ell} \propto & - \sum_{\lambda=\pm, 0} (H_{V, \lambda}^{\lambda_M} + H_{A, \lambda}^{\lambda_M}) L_{V-A, \lambda}^{\lambda_\ell} + (\tilde{H}_{V, t}^{\lambda_M} + \tilde{H}_{A, t}^{\lambda_M}) L_{V-A, t}^{\lambda_\ell} \\
& + 2 \sum_{\lambda=\pm} \left[(H_{T, \lambda 0}^{\lambda_M} + H_{T5, \lambda 0}^{\lambda_M}) L_{T-T5, \lambda 0}^{\lambda_\ell} - (H_{T, \lambda t}^{\lambda_M} + H_{T5, \lambda t}^{\lambda_M}) L_{T-T5, \lambda t}^{\lambda_\ell} \right] \\
& + 2(H_{T, +-}^{\lambda_M} + H_{T5, +-}^{\lambda_M}) L_{T-T5, +-}^{\lambda_\ell} - 2(H_{T, 0t}^{\lambda_M} + H_{T5, 0t}^{\lambda_M}) L_{T-T5, 0t}^{\lambda_\ell}.
\end{aligned} \tag{76}$$

Using the relations (75) one can write it in a more compact form :

$$\mathcal{M}^{\lambda_M, \lambda_\ell} \propto - \sum_{\lambda=\pm, 0} \tilde{H}_\lambda^{\lambda_M, \lambda_\ell} L_{V-A, \lambda}^{\lambda_\ell} + \tilde{H}_t^{\lambda_M} L_{V-A, t}^{\lambda_\ell}, \tag{77}$$

where the redefined amplitudes are given as,

$$\begin{aligned}
\tilde{H}_\pm^{\lambda_M, +} &\equiv H_{V, \pm}^{\lambda_M} + H_{A, \pm}^{\lambda_M} - 2 \frac{\sqrt{q^2}}{m_\ell} (H_{T, \pm t}^{\lambda_M} \pm H_{T, \pm 0}^{\lambda_M} + H_{T5, \pm t}^{\lambda_M} \pm H_{T5, \pm 0}^{\lambda_M}), \\
\tilde{H}_0^{\lambda_M, +} &\equiv H_{V, 0}^{\lambda_M} + H_{A, 0}^{\lambda_M} - 2 \frac{\sqrt{q^2}}{m_\ell} (H_{T, +-}^{\lambda_M} + H_{T, 0t}^{\lambda_M} + H_{T5, +-}^{\lambda_M} + H_{T5, 0t}^{\lambda_M}), \\
\tilde{H}_\pm^{\lambda_M, -} &\equiv H_{V, \pm}^{\lambda_M} + H_{A, \pm}^{\lambda_M} - 2 \frac{m_\ell}{\sqrt{q^2}} (H_{T, \pm t}^{\lambda_M} \pm H_{T, \pm 0}^{\lambda_M} + H_{T5, \pm t}^{\lambda_M} \pm H_{T5, \pm 0}^{\lambda_M}), \\
\tilde{H}_0^{\lambda_M, -} &\equiv H_{V, 0}^{\lambda_M} + H_{A, 0}^{\lambda_M} - 2 \frac{m_\ell}{\sqrt{q^2}} (H_{T, +-}^{\lambda_M} + H_{T, 0t}^{\lambda_M} + H_{T5, +-}^{\lambda_M} + H_{T5, 0t}^{\lambda_M}), \\
\tilde{H}_t^{\lambda_M} &\equiv \tilde{H}_{V, t}^{\lambda_M} + \tilde{H}_{A, t}^{\lambda_M}.
\end{aligned} \tag{78}$$

Absorbing the scalar and tensor amplitudes into \tilde{h} and \tilde{H} allows to significantly simplify the calculations and to write the expressions for the angular coefficients of the differential

decay rate in a much more compact way. To be more specific, we introduce the following linear combinations :

$$\begin{aligned}
\tilde{h}_0^+(q^2) &\equiv h_0(q^2) - 2\frac{\sqrt{q^2}}{m_\ell} h_T(q^2), \\
\tilde{h}_0^-(q^2) &\equiv h_0(q^2) - 2\frac{m_\ell}{\sqrt{q^2}} h_T(q^2), \\
\tilde{h}_t(q^2) &\equiv h_t(q^2) + \frac{\sqrt{q^2}}{m_\ell^2} h_S(q^2),
\end{aligned} \tag{79}$$

and

$$\begin{aligned}
\tilde{H}_\pm^+(q^2) &\equiv H_\pm(q^2) - 2\frac{\sqrt{q^2}}{m_\ell} H_{T,\pm}(q^2), \\
\tilde{H}_0^+(q^2) &\equiv H_0(q^2) - 2\frac{\sqrt{q^2}}{m_\ell} H_{T,0}(q^2), \\
\tilde{H}_\pm^-(q^2) &\equiv H_\pm(q^2) - 2\frac{m_\ell}{\sqrt{q^2}} H_{T,\pm}(q^2), \\
\tilde{H}_0^-(q^2) &\equiv H_0(q^2) - 2\frac{m_\ell}{\sqrt{q^2}} H_{T,0}(q^2), \\
\tilde{H}_t(q^2) &\equiv H_t(q^2) + \frac{\sqrt{q^2}}{m_\ell^2} H_P(q^2),
\end{aligned} \tag{80}$$

with

$$\begin{aligned}
h_T(q^2) &\equiv h_{T,0t}(q^2) + h_{T5,+}(q^2), \\
H_\pm(q^2) &\equiv H_{V,\pm}^\pm(q^2) + H_{A,\pm}^\pm(q^2), \\
H_{T,\pm}(q^2) &\equiv H_{T,\pm t}^\pm(q^2) \pm H_{T,\pm 0}^\pm(q^2) + H_{T5,\pm t}^\pm(q^2) \pm H_{T5,\pm 0}^\pm(q^2), \\
H_{T,0}(q^2) &\equiv H_{T,+}^0(q^2) + H_{T5,0t}^0(q^2).
\end{aligned} \tag{81}$$

To simplify and shorten the final expressions of angular observables, we omit the super-index λ_M in \tilde{h} and \tilde{H} .

Note that using the relations between various hadronic tensor amplitudes [Eqs. (68,69)], the tensor contribution to \tilde{h} and \tilde{H} in Eqs. (79,80) vanishes if $g_T = g_{T5}$. This is reasonable since the operator $\bar{c}\sigma_{\mu\nu}(1 + \gamma_5)b\bar{\ell}\sigma^{\mu\nu}(1 - \gamma_5)\nu$ identically vanishes due to the Fierz transformations.

C Polarization vectors and spinors

In the B rest frame the four-momenta of B (p), $D^{(*)}$ (k) and q are

$$p^\mu = \begin{pmatrix} m_B \\ 0 \\ 0 \\ 0 \end{pmatrix}, \quad k^\mu = \begin{pmatrix} E_{D^{(*)}} \\ 0 \\ 0 \\ |\mathbf{q}| \end{pmatrix}, \quad q^\mu = \begin{pmatrix} q_0 \\ 0 \\ 0 \\ -|\mathbf{q}| \end{pmatrix}. \tag{82}$$

The polarization vectors of D^* (ε) and the virtual vector boson (η) are defined in the B rest frame as in Ref. [74]:

$$\varepsilon^\mu(\pm) = \frac{1}{\sqrt{2}} \begin{pmatrix} 0 \\ \mp 1 \\ -i \\ 0 \end{pmatrix}, \quad \varepsilon^\mu(0) = \frac{1}{m_{D^*}} \begin{pmatrix} |\mathbf{q}| \\ 0 \\ 0 \\ E_{D^*} \end{pmatrix}, \quad (83)$$

and

$$\eta^\mu(\pm) = \frac{1}{\sqrt{2}} \begin{pmatrix} 0 \\ \mp 1 \\ i \\ 0 \end{pmatrix}, \quad \eta^\mu(0) = \frac{1}{\sqrt{q^2}} \begin{pmatrix} |\mathbf{q}| \\ 0 \\ 0 \\ -q_0 \end{pmatrix}, \quad \eta^\mu(t) = \frac{1}{\sqrt{q^2}} \begin{pmatrix} q_0 \\ 0 \\ 0 \\ -|\mathbf{q}| \end{pmatrix}, \quad (84)$$

with

$$|\mathbf{q}| = \frac{\sqrt{\lambda_{BD^*}(q^2)}}{2m_B}, \quad q_0 = \frac{m_B^2 - m_{D^*}^2 + q^2}{2m_B}, \quad E_{D^*} = \frac{m_B^2 + m_{D^*}^2 - q^2}{2m_B}. \quad (85)$$

Other alternative parametrization can be found in the seminal paper [75], in which the z -axis is also along $D^{(*)}$ momentum. Note that in Ref. [75] all four-vectors are defined as covariant, while in this work we define all vectors as contravariant.

The Dirac spinors, used in the leptonic helicity amplitudes (63) calculation, are defined as [74]

$$u(\lambda = \pm 1/2) = \begin{pmatrix} \sqrt{E \mp |\mathbf{p}|} \xi_\pm \\ \sqrt{E \pm |\mathbf{p}|} \xi_\pm \end{pmatrix}, \quad v(\lambda = \pm 1/2) = \begin{pmatrix} -\sqrt{E \pm |\mathbf{p}|} \xi_\mp \\ \sqrt{E \mp |\mathbf{p}|} \xi_\mp \end{pmatrix}, \quad (86)$$

where the helicity eigenspinors

$$\xi_+ = \begin{pmatrix} \cos \frac{\theta}{2} \\ \sin \frac{\theta}{2} e^{i\phi} \end{pmatrix}, \quad \xi_- = \begin{pmatrix} -\sin \frac{\theta}{2} e^{-i\phi} \\ \cos \frac{\theta}{2} \end{pmatrix}, \quad (87)$$

describe either particles of helicity $\pm 1/2$ respectively or antiparticles of helicity $\mp 1/2$. Since in this work we assume that neutrino is only left-handed, $\lambda_{\bar{\nu}} = 1/2$. The $\bar{\nu}$ spinor, $v(\lambda_{\bar{\nu}} = 1/2)$, is defined by Eqs. (86),(87) with $\theta_{\bar{\nu}} = \pi - \theta_\ell$ and $\phi_{\bar{\nu}} = \phi_\ell + \pi$. In our chosen system of coordinates the leptonic azimuthal angle $\phi_\ell \equiv \chi$.

D Four-body phase space

The four-body phase space can be reduced to the product of the two-body phase spaces:

$$\begin{aligned} d\Phi_4 &= (2\pi)^4 \int \prod_{i=1}^4 \frac{d^3 p_i}{(2\pi)^3 2E_i} \delta\left(P - \sum_{j=1}^4 p_j\right) \\ &= \frac{dm_{12}^2}{2\pi} \frac{dm_{34}^2}{2\pi} d\Phi_2(p_{12}, p_{34}) d\Phi_2(\hat{p}_1, \hat{p}_2) d\Phi_2(\hat{p}_3, \hat{p}_4), \end{aligned} \quad (88)$$

where $m_{ij}^2 = p_{ij}^2 = (p_i + p_j)^2$. The two-body phase space is given by the standard expression

$$d\Phi_2(\hat{p}_i, \hat{p}_j) = \frac{1}{16\pi^2} \frac{|\hat{p}_i|}{m_{ij}} d\cos\theta_i d\phi_i, \quad (89)$$

with three-momentum \hat{p}_i defined in the ij rest frame.

Using Eq. (88) one can write the phase space for the $\bar{B} \rightarrow D^*(\rightarrow D\pi)\ell\bar{\nu}_\ell$ as,

$$d\Phi_4 = \frac{1}{64(2\pi)^8} dm_{D\pi}^2 dq^2 \frac{|\hat{p}_{D\pi}|}{m_B} d\cos\theta_{D\pi} d\phi_{D\pi} \frac{|\hat{p}_D|}{m_{D\pi}} d\cos\theta_D d\phi_D \frac{|\hat{p}_\ell|}{\sqrt{q^2}} d\cos\theta_\ell d\phi_\ell, \quad (90)$$

where $\hat{p}_{D\pi}(= -\mathbf{q})$, \hat{p}_D , \hat{p}_ℓ and the corresponding angles are defined in the B , $D\pi$ and $\ell\bar{\nu}$ rest frames respectively, namely,

$$|\hat{p}_{D\pi}| = \frac{\sqrt{\lambda(m_B^2, m_{D\pi}^2, q^2)}}{2m_B}, \quad |\hat{p}_D| = \frac{\sqrt{\lambda(m_{D\pi}^2, m_D^2, m_\pi^2)}}{2m_{D\pi}}, \quad |\hat{p}_\ell| = \frac{q^2 - m_\ell^2}{2\sqrt{q^2}}, \quad (91)$$

where, as before, $\lambda(a, b, c) = a^2 + b^2 + c^2 - 2(ab + ac + bc)$.

Integrating over the polar and azimuthal angles of the D^* momentum ($\theta_{D\pi}$, $\phi_{D\pi}$) and over the azimuthal angle of the D momentum (ϕ_D), one obtains

$$d\Phi_4 = \frac{1}{64(2\pi)^6} \frac{|\mathbf{q}| |\hat{p}_D|}{m_B m_{D\pi}} \left(1 - \frac{m_\ell^2}{q^2}\right) dq^2 dm_{D\pi}^2 d\cos\theta_D d\cos\theta_\ell d\chi. \quad (92)$$

Here we defined the angle $\phi_\ell = \chi$ with respect to the $D\pi$ rest frame.

Similarly, one can obtain the three-body phase space for the $\bar{B} \rightarrow D\ell\bar{\nu}$ decay :

$$d\Phi_3 = \frac{dq^2}{2\pi} d\Phi_2(p_D, q) d\Phi_2(\hat{p}_\ell, \hat{p}_\nu) \rightarrow \frac{1}{16(2\pi)^3} \frac{|\mathbf{q}|}{m_B} \left(1 - \frac{m_\ell^2}{q^2}\right) dq^2 d\cos\theta_\ell. \quad (93)$$

E Fit results with NP couplings at best fit values

In here we show the fit results obtained following the same procedure as the one explained in Sec. 3.1, but fixing for each scenario the NP coupling at the best fit value, which can be found at Eqs. (45,46). Similarly to Tab. 2, these results have been obtained enforcing the experimental results for $R(D)$ and $R(D^*)$ and allowing for NP effects in one coefficient at a time. In particular, we show in Tab. 4 the results for the NP coefficients employed in Eq. (5), while we report in Tab. 5 the results for the ones introduced in Eq. (6). Since all the predicted observables behave in a Gaussian manner, we write for all of them the mean values and the standard deviations.

Obs.	Exp.	SM	g_V	g_A	g_S	g_P	g_T
R_D	0.334 ± 0.029	0.30 ± 0.02	0.40 ± 0.01	—	0.37 ± 0.02	—	0.33 ± 0.01
R_{D^*}	0.297 ± 0.015	0.258 ± 0.003	0.262 ± 0.003	0.299 ± 0.004	—	0.284 ± 0.006	0.30 ± 0.01
$R(A_{FB}^D)$	—	0.077 ± 0.004	0.071 ± 0.002	—	0.067 ± 0.002	—	0.081 ± 0.003
$R(A_{X_\ell}^D)$	—	-0.332 ± 0.003	-0.331 ± 0.003	—	-0.495 ± 0.003	—	-0.25 ± 0.05
$R(A_{X_\ell}^{D^*})$	—	0.47 ± 0.02	0.49 ± 0.02	0.48 ± 0.02	—	0.34 ± 0.03	0.22 ± 0.02
$R(R_{L,T})$	—	0.79 ± 0.02	0.76 ± 0.02	0.80 ± 0.02	—	0.99 ± 0.04	0.46 ± 0.02
$R(R_{A,B})$	—	0.520 ± 0.004	0.510 ± 0.004	0.524 ± 0.004	—	0.515 ± 0.004	0.613 ± 0.007
$R(A_{FB}^{D^*})$	—	0.23 ± 0.04	0.37 ± 0.03	-0.37 ± 0.04	—	-0.04 ± 0.04	-0.03 ± 0.03
$R(A_3)$	—	0.62 ± 0.01	0.58 ± 0.01	0.63 ± 0.01	—	0.55 ± 0.01	0.16 ± 0.07
$R(A_4)$	—	0.46 ± 0.01	0.45 ± 0.01	0.46 ± 0.01	—	0.41 ± 0.01	0.12 ± 0.04
$R(A_5)$	—	1.15 ± 0.02	1.24 ± 0.02	0.71 ± 0.03	—	1.27 ± 0.02	0.55 ± 0.05
$R(A_6)$	—	0.79 ± 0.01	0.92 ± 0.02	0.21 ± 0.01	—	0.71 ± 0.02	0.25 ± 0.05
$D(A_7)$	—	0	$(7.3 \pm 0.4) \cdot 10^{-3}$	0.035 ± 0.002	—	$(-5.6 \pm 0.2) \cdot 10^{-3}$	-0.02 ± 0.01
$D(A_8)$	—	0	$(5.2 \pm 0.2) \cdot 10^{-3}$	0.025 ± 0.001	—	0	0
$D(A_9)$	—	0	$(13.2 \pm 0.4) \cdot 10^{-3}$	0.063 ± 0.002	—	0	0

Table 4: All the observables obtained by using the values of the NP couplings given in Eq. 45.

Obs.	Exp.	SM	g_{V_L}	g_{V_R}	g_{S_L}	g_{S_R}
R_D	0.334 ± 0.029	0.30 ± 0.02	0.33 ± 0.01	0.33 ± 0.01	0.33 ± 0.01	0.37 ± 0.01
R_{D^*}	0.297 ± 0.014	0.258 ± 0.003	0.300 ± 0.004	0.300 ± 0.004	0.275 ± 0.005	0.263 ± 0.004
$R(A_{FB}^D)$	—	0.077 ± 0.004	0.074 ± 0.003	0.074 ± 0.003	0.044 ± 0.002	0.068 ± 0.002
$R(A_{X_\ell}^D)$	—	-0.332 ± 0.003	-0.331 ± 0.003	-0.331 ± 0.003	-0.403 ± 0.003	-0.501 ± 0.003
$R(A_{X_\ell}^{D*})$	—	0.47 ± 0.02	0.48 ± 0.02	0.48 ± 0.02	0.38 ± 0.02	0.44 ± 0.02
$R(R_{L,T})$	—	0.79 ± 0.02	0.79 ± 0.02	0.80 ± 0.02	0.92 ± 0.03	0.85 ± 0.02
$R(R_{A,B})$	—	0.520 ± 0.004	0.520 ± 0.004	0.520 ± 0.004	0.516 ± 0.004	0.519 ± 0.004
$R(A_{FB}^{D*})$	—	0.23 ± 0.04	0.23 ± 0.04	-0.02 ± 0.03	0.07 ± 0.04	0.13 ± 0.04
$R(A_3)$	—	0.62 ± 0.01	0.62 ± 0.01	0.62 ± 0.01	0.57 ± 0.01	0.60 ± 0.01
$R(A_4)$	—	0.46 ± 0.01	0.455 ± 0.005	0.455 ± 0.005	0.41 ± 0.01	0.45 ± 0.01
$R(A_5)$	—	1.15 ± 0.02	1.16 ± 0.02	1.00 ± 0.02	1.19 ± 0.02	1.02 ± 0.02
$R(A_6)$	—	0.79 ± 0.01	0.79 ± 0.01	0.57 ± 0.02	0.73 ± 0.01	0.77 ± 0.01
$D(A_7)$	—	0	0	-0.027 ± 0.001	0.019 ± 0.001	$(-2.2 \pm 0.1) \cdot 10^{-3}$
$D(A_8)$	—	0	0	-0.019 ± 0.001	0	0
$D(A_9)$	—	0	0	-0.047 ± 0.001	0	0

Table 5: Same as in Tab. 4 but in different basis of operators and for values of NP couplings given in Eq. 46.

References

- [1] **BaBar** Collaboration, B. Aubert *et al.*, “Observation of the semileptonic decays $B \rightarrow D^* \tau^- \bar{\nu}(\tau)$ and evidence for $B \rightarrow D \tau^- \bar{\nu}(\tau)$ ”, *Phys. Rev. Lett.* **100** (2008) 021801, [arXiv:0709.1698 \[hep-ex\]](#).
- [2] **BaBar** Collaboration, J. P. Lees *et al.*, “Evidence for an excess of $\bar{B} \rightarrow D^{(*)} \tau^- \bar{\nu}_\tau$ decays”, *Phys. Rev. Lett.* **109** (2012) 101802, [arXiv:1205.5442 \[hep-ex\]](#).
- [3] **Belle** Collaboration, M. Huschle *et al.*, “Measurement of the branching ratio of $\bar{B} \rightarrow D^{(*)} \tau^- \bar{\nu}_\tau$ relative to $\bar{B} \rightarrow D^{(*)} \ell^- \bar{\nu}_\ell$ decays with hadronic tagging at Belle”, *Phys. Rev.* **D92** (2015) no. 7, 072014, [arXiv:1507.03233 \[hep-ex\]](#).
- [4] **Belle** Collaboration, Y. Sato *et al.*, “Measurement of the branching ratio of $\bar{B}^0 \rightarrow D^{*+} \tau^- \bar{\nu}_\tau$ relative to $\bar{B}^0 \rightarrow D^{*+} \ell^- \bar{\nu}_\ell$ decays with a semileptonic tagging method”, *Phys. Rev.* **D94** (2016) no. 7, 072007, [arXiv:1607.07923 \[hep-ex\]](#).
- [5] **LHCb** Collaboration, R. Aaij *et al.*, “Measurement of the ratio of branching fractions $\mathcal{B}(\bar{B}^0 \rightarrow D^{*+} \tau^- \bar{\nu}_\tau) / \mathcal{B}(\bar{B}^0 \rightarrow D^{*+} \mu^- \bar{\nu}_\mu)$ ”, *Phys. Rev. Lett.* **115** (2015) no. 11, 111803, [arXiv:1506.08614 \[hep-ex\]](#). [Erratum: *Phys. Rev. Lett.* 115, no. 15, 159901 (2015)].
- [6] **LHCb** Collaboration, R. Aaij *et al.*, “Measurement of the ratio of the $B^0 \rightarrow D^{*-} \tau^+ \nu_\tau$ and $B^0 \rightarrow D^{*-} \mu^+ \nu_\mu$ branching fractions using three-prong τ -lepton decays”, *Phys. Rev. Lett.* **120** (2018) no. 17, 171802, [arXiv:1708.08856 \[hep-ex\]](#).
- [7] S. Fajfer, J. F. Kamenik, and I. Nisandzic, “On the $B \rightarrow D^* \tau \bar{\nu}_\tau$ Sensitivity to New Physics”, *Phys. Rev.* **D85** (2012) 094025, [arXiv:1203.2654 \[hep-ph\]](#).
- [8] F. U. Bernlochner, Z. Ligeti, M. Papucci, and D. J. Robinson, “Combined analysis of semileptonic B decays to D and D^* : $R(D^{(*)})$, $|V_{cb}|$, and new physics”, *Phys. Rev.* **D95** (2017) no. 11, 115008, [arXiv:1703.05330 \[hep-ph\]](#). [Erratum: *Phys. Rev.* D97, no. 5, 059902 (2018)].
- [9] S. Jaiswal, S. Nandi, and S. K. Patra, “Extraction of $|V_{cb}|$ from $B \rightarrow D^{(*)} \ell \nu_\ell$ and the Standard Model predictions of $R(D^{(*)})$ ”, *JHEP* **12** (2017) 060, [arXiv:1707.09977 \[hep-ph\]](#).
- [10] P. Gambino, M. Jung, and S. Schacht, “The V_{cb} puzzle: an update”, [arXiv:1905.08209 \[hep-ph\]](#).
- [11] R.-X. Shi, L.-S. Geng, B. Grinstein, S. Jäger, and J. Martin Camalich, “Revisiting the new-physics interpretation of the $b \rightarrow c \tau \nu$ data”, [arXiv:1905.08498 \[hep-ph\]](#).

- [12] M. Blanke, A. Crivellin, T. Kitahara, M. Moscati, U. Nierste, and I. Nišandžić, “Addendum: ”Impact of polarization observables and $B_c \rightarrow \tau\nu$ on new physics explanations of the $b \rightarrow c\tau\nu$ anomaly””, [arXiv:1905.08253 \[hep-ph\]](#).
- [13] C. Murgui, A. Peñuelas, M. Jung, and A. Pich, “Global fit to $b \rightarrow c\tau\nu$ transitions””, [arXiv:1904.09311 \[hep-ph\]](#).
- [14] O. Popov, M. A. Schmidt, and G. White, “ R_2 as a single leptoquark solution to $R_{D^{(*)}}$ and $R_{K^{(*)}}$ ”, [arXiv:1905.06339 \[hep-ph\]](#).
- [15] C. Cornella, J. Fuentes-Martin, and G. Isidori, “Revisiting the vector leptoquark explanation of the B-physics anomalies””, [arXiv:1903.11517 \[hep-ph\]](#).
- [16] A. K. Alok, D. Kumar, S. Kumbhakar, and S. Uma Sankar, “Impact of D^* polarization measurement on solutions to R_D - R_{D^*} anomalies””, [arXiv:1903.10486 \[hep-ph\]](#).
- [17] M. Blanke, A. Crivellin, S. de Boer, T. Kitahara, M. Moscati, U. Nierste, and I. Nišandžić, “Impact of polarization observables and $B_c \rightarrow \tau\nu$ on new physics explanations of the $b \rightarrow c\tau\nu$ anomaly””, *Phys. Rev.* **D99** (2019) no. 7, 075006, [arXiv:1811.09603 \[hep-ph\]](#).
- [18] S. Iguro, T. Kitahara, Y. Omura, R. Watanabe, and K. Yamamoto, “ D^* polarization vs. $R_{D^{(*)}}$ anomalies in the leptoquark models””, *JHEP* **02** (2019) 194, [arXiv:1811.08899 \[hep-ph\]](#).
- [19] J. Aebischer, J. Kumar, P. Stangl, and D. M. Straub, “A Global Likelihood for Precision Constraints and Flavour Anomalies””, [arXiv:1810.07698 \[hep-ph\]](#).
- [20] Q.-Y. Hu, X.-Q. Li, and Y.-D. Yang, “ $b \rightarrow c\tau\nu$ transitions in the standard model effective field theory””, *Eur. Phys. J.* **C79** (2019) no. 3, 264, [arXiv:1810.04939 \[hep-ph\]](#).
- [21] A. Angelescu, D. Becirevic, D. A. Faroughy, and O. Sumensari, “Closing the window on single leptoquark solutions to the B -physics anomalies””, *JHEP* **10** (2018) 183, [arXiv:1808.08179 \[hep-ph\]](#).
- [22] J. Heeck and D. Teresi, “Pati-Salam explanations of the B-meson anomalies””, *JHEP* **12** (2018) 103, [arXiv:1808.07492 \[hep-ph\]](#).
- [23] T. Faber, M. Hudec, M. Malinský, P. Meinzinger, W. Porod, and F. Staub, “A unified leptoquark model confronted with lepton non-universality in B -meson decays””, *Phys. Lett.* **B787** (2018) 159–166, [arXiv:1808.05511 \[hep-ph\]](#).

- [24] Z.-R. Huang, Y. Li, C.-D. Lu, M. A. Paracha, and C. Wang, “Footprints of New Physics in $b \rightarrow c\tau\nu$ Transitions”, *Phys. Rev.* **D98** (2018) no. 9, 095018, [arXiv:1808.03565 \[hep-ph\]](#).
- [25] F. Feruglio, P. Paradisi, and O. Sumensari, “Implications of scalar and tensor explanations of $R_{D^{(*)}}$ ”, *JHEP* **11** (2018) 191, [arXiv:1806.10155 \[hep-ph\]](#).
- [26] D. Becirevic, I. Doršner, S. Fajfer, N. Košnik, D. A. Faroughy, and O. Sumensari, “Scalar leptoquarks from grand unified theories to accommodate the B -physics anomalies”, *Phys. Rev.* **D98** (2018) no. 5, 055003, [arXiv:1806.05689 \[hep-ph\]](#).
- [27] M. Bordone, C. Cornella, J. Fuentes-Martín, and G. Isidori, “Low-energy signatures of the PS^3 model: from B -physics anomalies to LFV”, *JHEP* **10** (2018) 148, [arXiv:1805.09328 \[hep-ph\]](#).
- [28] A. Azatov, D. Bardhan, D. Ghosh, F. Sgarlata, and E. Venturini, “Anatomy of $b \rightarrow c\tau\nu$ anomalies”, *JHEP* **11** (2018) 187, [arXiv:1805.03209 \[hep-ph\]](#).
- [29] A. K. Alok, D. Kumar, S. Kumbhakar, and S. Uma Sankar, “Resolution of R_D/R_{D^*} puzzle”, *Phys. Lett.* **B784** (2018) 16–20, [arXiv:1804.08078 \[hep-ph\]](#).
- [30] D. Marzocca, “Addressing the B-physics anomalies in a fundamental Composite Higgs Model”, *JHEP* **07** (2018) 121, [arXiv:1803.10972 \[hep-ph\]](#).
- [31] M. Blanke and A. Crivellin, “ B Meson Anomalies in a Pati-Salam Model within the Randall-Sundrum Background”, *Phys. Rev. Lett.* **121** (2018) no. 1, 011801, [arXiv:1801.07256 \[hep-ph\]](#).
- [32] M. Jung and D. M. Straub, “Constraining new physics in $b \rightarrow c\ell\nu$ transitions”, *JHEP* **01** (2019) 009, [arXiv:1801.01112 \[hep-ph\]](#).
- [33] A. K. Alok, D. Kumar, J. Kumar, S. Kumbhakar, and S. U. Sankar, “New physics solutions for R_D and R_{D^*} ”, *JHEP* **09** (2018) 152, [arXiv:1710.04127 \[hep-ph\]](#).
- [34] D. Buttazzo, A. Greljo, G. Isidori, and D. Marzocca, “B-physics anomalies: a guide to combined explanations”, *JHEP* **11** (2017) 044, [arXiv:1706.07808 \[hep-ph\]](#).
- [35] W. Altmannshofer, P. S. Bhupal Dev, and A. Soni, “ $R_{D^{(*)}}$ anomaly: A possible hint for natural supersymmetry with R -parity violation”, *Phys. Rev.* **D96** (2017) no. 9, 095010, [arXiv:1704.06659 \[hep-ph\]](#).
- [36] A. Crivellin, D. Müller, and T. Ota, “Simultaneous explanation of $R(D^{(*)})$ and $b \rightarrow s\mu^+\mu^-$: the last scalar leptoquarks standing”, *JHEP* **09** (2017) 040, [arXiv:1703.09226 \[hep-ph\]](#).

- [37] A. Celis, M. Jung, X.-Q. Li, and A. Pich, “Scalar contributions to $b \rightarrow c(u)\tau\nu$ transitions”, *Phys. Lett.* **B771** (2017) 168–179, [arXiv:1612.07757 \[hep-ph\]](#).
- [38] R. Alonso, A. Kobach, and J. Martin Camalich, “New physics in the kinematic distributions of $\bar{B} \rightarrow D^{(*)}\tau^-(\rightarrow \ell^-\bar{\nu}_\ell\nu_\tau)\bar{\nu}_\tau$ ”, *Phys. Rev.* **D94** (2016) no. 9, 094021, [arXiv:1602.07671 \[hep-ph\]](#).
- [39] M. Freytsis, Z. Ligeti, and J. T. Ruderman, “Flavor models for $\bar{B} \rightarrow D^{(*)}\tau\bar{\nu}$ ”, *Phys. Rev.* **D92** (2015) no. 5, 054018, [arXiv:1506.08896 \[hep-ph\]](#).
- [40] A. Abada, A. M. Teixeira, A. Vicente, and C. Weiland, “Sterile neutrinos in leptonic and semileptonic decays”, *JHEP* **02** (2014) 091, [arXiv:1311.2830 \[hep-ph\]](#).
- [41] M. Tanaka and R. Watanabe, “New physics in the weak interaction of $\bar{B} \rightarrow D^{(*)}\tau\bar{\nu}$ ”, *Phys. Rev.* **D87** (2013) no. 3, 034028, [arXiv:1212.1878 \[hep-ph\]](#).
- [42] S. Trifinopoulos, “B-physics anomalies: The bridge between R-parity violating Supersymmetry and flavoured Dark Matter”, [arXiv:1904.12940 \[hep-ph\]](#).
- [43] **Belle** Collaboration, A. Abdesselam *et al.*, “Measurement of $\mathcal{R}(D)$ and $\mathcal{R}(D^*)$ with a semileptonic tagging method”, [arXiv:1904.08794 \[hep-ex\]](#).
- [44] **HFLAV** Collaboration, Y. Amhis *et al.*, “Averages of b -hadron, c -hadron, and τ -lepton properties as of summer 2016”, *Eur. Phys. J.* **C77** (2017) no. 12, 895, [arXiv:1612.07233 \[hep-ex\]](#).
- [45] A. V. Avilés-Casco, C. DeTar, A. X. El-Khadra, A. S. Kronfeld, J. Laiho, and R. S. Van de Water, “ $B \rightarrow D^*\ell\nu$ at non-zero recoil”, *PoS LATTICE2018* (2019) 282, [arXiv:1901.00216 \[hep-lat\]](#).
- [46] A. Vaquero, C. DeTar, A. X. El-Khadra, A. S. Kronfeld, J. Laiho, and R. S. Van de Water, “ $B \rightarrow D^*\ell\nu$ at non-zero recoil”, in *17th Conference on Flavor Physics and CP Violation (FPCP 2019) Victoria, BC, Canada, May 6-10, 2019*. 2019. [arXiv:1906.01019 \[hep-lat\]](#).
- [47] **MILC** Collaboration, J. A. Bailey *et al.*, “ $B \rightarrow D\ell\nu$ form factors at nonzero recoil and $|V_{cb}|$ from 2+1-flavor lattice QCD”, *Phys. Rev.* **D92** (2015) no. 3, 034506, [arXiv:1503.07237 \[hep-lat\]](#).
- [48] **HPQCD** Collaboration, J. Harrison, C. Davies, and M. Wingate, “Lattice QCD calculation of the $B_{(s)} \rightarrow D_{(s)}^*\ell\nu$ form factors at zero recoil and implications for $|V_{cb}|$ ”, *Phys. Rev.* **D97** (2018) no. 5, 054502, [arXiv:1711.11013 \[hep-lat\]](#).
- [49] M. Atoui, V. Morénas, D. Bečirević, and F. Sanfilippo, “ $B_s \rightarrow D_s\ell\nu_\ell$ near zero recoil in and beyond the Standard Model”, *Eur. Phys. J.* **C74** (2014) no. 5, 2861, [arXiv:1310.5238 \[hep-lat\]](#).

- [50] S. de Boer, T. Kitahara, and I. Nisandzic, “Soft-Photon Corrections to $\bar{B} \rightarrow D\tau^-\bar{\nu}_\tau$ Relative to $\bar{B} \rightarrow D\mu^-\bar{\nu}_\mu$ ”, *Phys. Rev. Lett.* **120** (2018) no. 26, 261804, [arXiv:1803.05881 \[hep-ph\]](#).
- [51] D. Becirevic and N. Kosnik, “Soft photons in semileptonic $B \rightarrow D$ decays”, *Acta Phys. Polon. Supp.* **3** (2010) 207–214, [arXiv:0910.5031 \[hep-ph\]](#).
- [52] **LHCb** Collaboration, R. Aaij *et al.*, “Measurement of the ratio of branching fractions $\mathcal{B}(B_c^+ \rightarrow J/\psi\tau^+\nu_\tau)/\mathcal{B}(B_c^+ \rightarrow J/\psi\mu^+\nu_\mu)$ ”, *Phys. Rev. Lett.* **120** (2018) no. 12, 121801, [arXiv:1711.05623 \[hep-ex\]](#).
- [53] P. Colangelo and F. De Fazio, “Scrutinizing $\bar{B} \rightarrow D^*(D\pi)\ell^-\bar{\nu}_\ell$ and $\bar{B} \rightarrow D^*(D\gamma)\ell^-\bar{\nu}_\ell$ in search of new physics footprints”, *JHEP* **06** (2018) 082, [arXiv:1801.10468 \[hep-ph\]](#).
- [54] P. Biancofiore, P. Colangelo, and F. De Fazio, “On the anomalous enhancement observed in $B \rightarrow D^{(*)}\tau\bar{\nu}_\tau$ decays”, *Phys. Rev.* **D87** (2013) no. 7, 074010, [arXiv:1302.1042 \[hep-ph\]](#).
- [55] S. Faller, T. Mannel, and S. Turczyk, “Limits on New Physics from exclusive $B \rightarrow D^{(*)}\ell\bar{\nu}$ Decays”, *Phys. Rev.* **D84** (2011) 014022, [arXiv:1105.3679 \[hep-ph\]](#).
- [56] D. Becirevic, S. Fajfer, I. Nisandzic, and A. Tayduganov, “Angular distributions of $\bar{B} \rightarrow D^{(*)}\ell\bar{\nu}_\ell$ decays and search of New Physics”, [arXiv:1602.03030 \[hep-ph\]](#).
- [57] S. Bhattacharya, S. Nandi, and S. K. Patra, “Optimal-observable analysis of possible new physics in $B \rightarrow D^{(*)}\tau\nu_\tau$ ”, *Phys. Rev.* **D93** (2016) no. 3, 034011, [arXiv:1509.07259 \[hep-ph\]](#).
- [58] M. A. Ivanov, J. G. Körner, and C. T. Tran, “Exclusive decays $B \rightarrow \ell^-\bar{\nu}$ and $B \rightarrow D^{(*)}\ell^-\bar{\nu}$ in the covariant quark model”, *Phys. Rev.* **D92** (2015) no. 11, 114022, [arXiv:1508.02678 \[hep-ph\]](#).
- [59] Y. Sakaki, M. Tanaka, A. Tayduganov, and R. Watanabe, “Probing New Physics with q^2 distributions in $\bar{B} \rightarrow D^{(*)}\tau\bar{\nu}$ ”, *Phys. Rev.* **D91** (2015) no. 11, 114028, [arXiv:1412.3761 \[hep-ph\]](#).
- [60] Y. Sakaki, M. Tanaka, A. Tayduganov, and R. Watanabe, “Testing leptoquark models in $\bar{B} \rightarrow D^{(*)}\tau\bar{\nu}$ ”, *Phys. Rev.* **D88** (2013) no. 9, 094012, [arXiv:1309.0301 \[hep-ph\]](#).
- [61] T. D. Cohen, H. Lamm, and R. F. Lebed, “Tests of the standard model in $B \rightarrow D\ell\nu_\ell$, $B \rightarrow D^*\ell\nu_\ell$ and $B_c \rightarrow J/\Psi\ell\nu_\ell$ ”, *Phys. Rev.* **D98** (2018) no. 3, 034022, [arXiv:1807.00256 \[hep-ph\]](#).

- [62] “Hepfit, a tool to combine indirect and direct constraints on high energy physics.” <http://hepfit.roma1.infn.it/>.
- [63] D. Melikhov and B. Stech, “Weak form-factors for heavy meson decays: An Update”, *Phys.Rev.* **D62** (2000) 014006, [arXiv:hep-ph/0001113 \[hep-ph\]](#).
- [64] I. Caprini, L. Lellouch, and M. Neubert, “Dispersive bounds on the shape of $\bar{B} \rightarrow D^{(*)} \ell \bar{\nu}$ form-factors”, *Nucl.Phys.* **B530** (1998) 153–181, [arXiv:hep-ph/9712417 \[hep-ph\]](#).
- [65] C. G. Boyd, B. Grinstein, and R. F. Lebed, “Precision corrections to dispersive bounds on form-factors”, *Phys. Rev.* **D56** (1997) 6895–6911, [arXiv:hep-ph/9705252 \[hep-ph\]](#).
- [66] D. Bigi, P. Gambino, and S. Schacht, “A fresh look at the determination of $|V_{cb}|$ from $B \rightarrow D^* \ell \nu$ ”, *Phys. Lett.* **B769** (2017) 441–445, [arXiv:1703.06124 \[hep-ph\]](#).
- [67] Belle Collaboration, A. Abdesselam *et al.*, “Measurement of CKM Matrix Element $|V_{cb}|$ from $\bar{B} \rightarrow D^{*+} \ell^- \bar{\nu}_\ell$ ”, [arXiv:1809.03290 \[hep-ex\]](#).
- [68] Flavour Lattice Averaging Group Collaboration, S. Aoki *et al.*, “FLAG Review 2019”, [arXiv:1902.08191 \[hep-lat\]](#).
- [69] X.-Q. Li, Y.-D. Yang, and X. Zhang, “Revisiting the one leptoquark solution to the $R(D^{(*)})$ anomalies and its phenomenological implications”, *JHEP* **08** (2016) 054, [arXiv:1605.09308 \[hep-ph\]](#).
- [70] R. Alonso, B. Grinstein, and J. Martin Camalich, “Lifetime of B_c^- Constrains Explanations for Anomalies in $B \rightarrow D^{(*)} \tau \nu$ ”, *Phys. Rev. Lett.* **118** (2017) no. 8, 081802, [arXiv:1611.06676 \[hep-ph\]](#).
- [71] C. McNeile, C. T. H. Davies, E. Follana, K. Hornbostel, and G. P. Lepage, “Heavy meson masses and decay constants from relativistic heavy quarks in full lattice QCD”, *Phys. Rev.* **D86** (2012) 074503, [arXiv:1207.0994 \[hep-lat\]](#).
- [72] Belle Collaboration, A. Abdesselam *et al.*, “Measurement of the D^{*-} polarization in the decay $B^0 \rightarrow D^{*-} \tau^+ \nu_\tau$ ”, in *10th International Workshop on the CKM Unitarity Triangle (CKM 2018) Heidelberg, Germany, September 17-21, 2018*. 2019. [arXiv:1903.03102 \[hep-ex\]](#).
- [73] D. Bečirević, N. Košnik, O. Sumensari, and R. Zukanovich Funchal, “Palatable Leptoquark Scenarios for Lepton Flavor Violation in Exclusive $b \rightarrow s \ell_1 \ell_2$ modes”, *JHEP* **11** (2016) 035, [arXiv:1608.07583 \[hep-ph\]](#).

- [74] K. Hagiwara, A. D. Martin, and M. F. Wade, “Exclusive semileptonic B meson decays”, *Nucl. Phys.* **B327** (1989) 569–594.
- [75] J. G. Korner and G. A. Schuler, “Exclusive Semileptonic Heavy Meson Decays Including Lepton Mass Effects”, *Z. Phys.* **C46** (1990) 93.